PLANE ELECTROMAGNETIC WAVE SCATTERING BY A COATED PERFECTLY CONDUCTING CYLINDER

by

IKE YI CHANG, JR.

Submitted to the

DEPARTMENT OF

ELECTRICAL ENGINEERING AND COMPUTER SCIENCE

in Partial Fulfillment of the Requirements for the Degrees of

BACHELOR OF SCIENCE

and

MASTER OF SCIENCE

at the

MASSACHUSETTS INSTITUTE OF TECHNOLOGY

May 1989

Signature of Author _____

Department of Electrical Engineering and Computer Science
May, 1989

Certified by _____

Professor Jin Au Kong
Thesis Supervisor

Certified by _____

Dr. Robert T. Shin
Company Supervisor

Accepted by _____

Professor Arthur C. Smith, Chairman
Committee on Graduate Students

PLANE ELECTROMAGNETIC WAVE SCATTERING

BY A

COATED PERFECTLY CONDUCTING CYLINDER

by

IKE YI CHANG, JR.

Submitted to the Department of Electrical Engineering and Computer Science
in Partial Fulfillment of the Requirements for the Degrees of
Bachelor of Science and Master of Science

ABSTRACT

Solutions to plane electromagnetic wave scattering by a coated perfectly conducting cylinder will be investigated. Cylindrical structures serve as a model for the study of radio wave diffraction over the earth and radar cross section prediction. An eigenfunction series solution can be obtained by matching tangential $\overline{E}$ and $\overline{H}$-fields of solutions to Maxwell's equations in the coating and air. Unfortunately, the eigenfunction solution converges slowly at high frequencies, when free space wavelength is small compared to cylinder radius. The Watson Transformation is used to convert the eigenfunction series into an integral solution. This integral can be solved using the stationary phase approximation, yielding a solution in the illuminated region that contains the incident field and specular reflections. The specular field is expressed as the incident field multiplied by a reflection coefficient and "spread factor."

In addition, the integral solution is evaluated by deforming the contour and picking up the pole contributions. This gives an exact residue series solution that is quickly convergent at high frequencies. The expression for each term of the residue series yields a mode amplitude and a propagation constant for the corresponding mode. The total diffracted field is the sum of the radiation due to all of the modes. The residue series solution is used for calculation of the multiply encircling creeping waves. The exact residue series, while converging quickly at high frequencies, poses difficulties in its numerical computation because it requires the computation of Bessel functions of complex order and complex argument. An alternative to the exact residue series solution is an approximate residue solution formulated by Habashy. The approximated solution avoids many computational difficulties encountered when solving for the exact solution directly. Finally, asymptotic approximations of Hankel functions are applied to recast the approximate residue series solution into a ray optics format. Test cases are presented that compare the results from the eigenfunction, specular, and exact and approximate residue series solutions.

Thesis Supervisor: Jin Au Kong
Professor of Electrical Engineering

Company Supervisor: Dr. Robert T. Shin
Staff Member, MIT Lincoln Laboratory

ACKNOWLEDGEMENTS

I wish to thank Dr. Robert Shin for his patience and effort in supervising this thesis. I also want to thank Professor Jin Au Kong for his helpful support and his group has been a pleasurable learning experience.

In addition, I thank my colleagues Eric Yang, Simon Yueh, Cheung Wei Lam, David Sheen, David Arnold, Jake Xia, Dieter Rebholz, Dr. Sami Ali, Hsiu Han, Michael Tsuk, and Son Nghiem for their frankness and eagerness to help whenever I ask. I also thank Nelson Chu, Dan Wang, Bob Atkins, Check Lee, Judy Chen, Freeman Lin, Ann Tulintseff, and Harold Lim for their warm friendship inside as well as outside the workplace.

Most of all, I thank my parents for their unconditional love and encouragement.

This Thesis is Dedicated to Dr. Ike Chang and Professor Imogene Chang...

whom I consider my best friends as much as my parents.

TABLE OF CONTENTS

LIST OF FIGURES

CHAPTER 1

INTRODUCTION

Scattering of electromagnetic waves by a coated perfectly conducting cylinder has many applications. In the 1940s and 50s, the scattering of cylindrical structures served as a model to study the phenomena of diffraction of radio waves over the earth. The study of creeping wave diffraction is also helpful in understanding the coupling of antennas lying on a curved surface [29]. More recently, scattering of coated cylinders has been of great interest in the field of radar cross section prediction because many objects of interest can be adequately modelled as cylinders. One particular application is the study of the effects of dielectric coating on the radar cross section of re-entry vehicles or aircraft [19]. Furthermore, approximate as well as exact solutions of canonical shapes such as cylinders have lead to the scattering solutions of more complex shapes.

The objective of this thesis is to examine various electromagnetic plane wave scattering solutions by coated perfectly conducting cylinders. Elliot [4] has derived an exact eigenfunction series solution by matching boundary conditions on solutions to Maxwell Equations. The eigenfunction series may provide adequate results for low frequency, when wavelength is comparable to the radius of the cylinder. Unfortunately, the eigenfunction series is slowly convergent for higher frequencies. Numerous papers discuss various high frequency solutions to cylinder scattering. Wu [38] has solved the scattering of a cylinder and sphere in the limit of small wavelength using asymptotic expansion techniques for the perfectly conducting case. Wang [36] has approached the

high-frequency problem by modelling the coated cylinder as a cylinder with constant impedance boundary condition. This latter approach has yielded fairly accurate results for cylinders with moderate coating thicknesses, but loses accuracy as coating thickness becomes comparable with the cylinder radius.

To obtain a quickly convergent exact solution for higher frequencies, Habashy [11] and Wang [36-7] employ the Watson Transformation. The Watson Transformation converts the eigenfunction series into a residue series. Next, the residue series is equated with a contour integral enclosing the upper half plane, which is then converted back into another residue series solution as a function of the order of the Bessel functions in the equation. This final residue series is quickly convergent at higher frequencies. The poles of the residues correspond to the resonant modes of the cylinder. Thus, total scattering can be expressed as the sum of the scattering due to all of the resonant modes of the structure [11].

For the residue series solutions, separate solutions apply to the illuminated region and the shadow region. The solution is presented in a format similar to that of the Geometrical Theory of Diffraction (GTD) formulated by Keller [16]. In the illuminated region, scattering is attributed to a specular reflection term plus a diffraction term due to multiply encircling creeping waves. Earlier, Keller [17] had derived a simple formula for the reflected and diffracted field by applying the theory of geometrical optics. More sophisticated approximate solutions for the specular field have been derived by Kim [18] and Helstrom [13] using the stationary phase approximation. The specular field is expressed as the incident field at the specular point multiplied by a reflection coefficient and "spread factor." In general, almost all of the scattering in the illuminated region is due to the specular field. Thus, in most cases, an approximate formula for the

specular field alone accurately predicts scattering in the illuminated region. In cases where there is resonance, i.e. one of the modes has low attenuation and appreciable amplitude, the lowest order resonant creeping wave mode assumes a larger role in the scattering solution. In this case, the creeping wave must be added on to the specular field to yield an accurate result.

In the shadow region, the specular field makes no contribution to scattering and only the diffracted field in the form of creeping waves exists. Creeping wave contributions are mathematically expressed in terms of the sum of the radiation due to each mode propagating on the cylinder. In the GTD ray format, creeping waves are created when an incident ray strikes the coating surface and generates a ray that azimuthally "creeps" around the air-coating surface of the cylinder. The location of the poles of the residue series defines the propagation constants of the creeping wave modes, which determine the phase velocity and attenuation. These poles, called Regge poles, are calculated as the roots of the denominator of the expression resulting from the Watson Transformation. This requires the finding of roots of a transcendental equation containing cylindrical Bessel functions of complex order as well as complex argument. Wang [37] and Paknys [25] have calculated the propagation constants of the excited creeping wave modes for an impedance cylinder by numerically solving such a transcendental equation. Paknys [26], Wang [36], and Kim [18] have gone further to calculate roots and present plots describing the trajectories of the Regge poles for a dielectric coated cylinder.

The coefficients of the residue series define the radiation amplitude of the creeping wave modes. An exact solution for the residue series gives highly accurate results in the deep shadow region. Unfortunately, the numerical computation of the series coefficients

using the exact equation is difficult and cumbersome. The impedance model simplifies the expression for the residue series coefficients and yields accurate results for thin coatings whose thickness is small compared to the radius of curvature. Paknys' analysis [26] of the impedance of the coated cylinder gives insight into resonance phenomena, when the creeping wave attenuation is very low. As is shown in Paknys [25-27], the creeping wave at resonance represents a coupling of the high attenuation creeping wave with the low attenuation guided wave associated with the planar dielectric slab backed by a ground plane.

Yet another solution has been formulated by Habashy [11], in which various asymptotic approximations are employed in the residue series equation to arrive at an approximate form of the residue series solution. As part of the high-frequency analysis, Habashy also examines the creeping wave case from a guided wave point of view, and thus solves for the diffracted field at resonance. This is accomplished by first looking at the guidance condition of modes in a flat dielectric slab backed by a ground plane. The coated cylinder idthen treated as a perturbation of the flat slab case, where the perturbation is due to the curvature of the cylinder.

Further work in this area includes the scattering solution in the transition region, the narrow region representing the "twilight" between the illuminated and shadow region. This work is necessary because both the formulation for the specular field in the lit region and the residue series of the creeping wave in the shadow region diverge in the transition region. Kim [18] has derived a solution based on Fock-type Airy functions in the formalism of Pathak's Uniform Theory of Diffraction (UTD) [28]. Other work includes Kato's [15] derivation of the specular and diffracted fields for a plane wave incident upon a coated conducting cylinder at oblique angles of incidence.

In Chapter 2, three exact scattering solutions from a coated perfectly conducting cylinder are derived. By expressing the field inside and outside the coating as sums of cylindrical harmonics, the eigenfunction series solution for TE and TM polarized are obtained by matching boundary conditions. To obtain solutions convergent for high frequency, the Watson Transformation is used to convert the eigenfunction series into an integral solution. Using contour integral methods, a residue series solution is derived. The latter yields an exact expression for creeping waves and total field in the shadow region.

In Chapter 3, the integral solution from Chapter 2 is cast into the GTD ray format. Scattering is expressed by two expressions, one valid in the illuminated region, the other in the shadow region. The expression in the illuminated region can be further divided into two parts. The first part is solved using stationary phase approximations. The result equals the incident field plus the specular reflections. The second part of the expression can be solved by deforming the contour and picking up the residues. This gives the creeping wave diffraction in the illuminated region. Thus, the entire field in the illuminated region equals the sum of the incident field, reflected field, and creeping waves. In the shadow region, the incident field is eclipsed by the cylinder. Therefore the entire field in the shadow region consists only of the creeping waves, and the residue series sufficiently calculates the field in the shadow region. Test cases are presented which compare the results from the GTD specular solution and the eigenfunction series solution.

In Chapter 4, an approximate formulation to the residue series solution is presented. Using various asymptotic expansions of the Hankel functions, the approximate formulation converts the modal and amplitude equations into a simpler form involving

Airy functions. The residue series solution converges quite rapidly for higher frequencies because the attenuation coefficients increase rapidly with mode number. Thus, only a few terms in the residue series are necessary for an accurate result. Test cases compare the results of the exact and approximation residue series solutions with those of the exact eigenfunction solution.

In Chapter 5, the work in this thesis is summarized and some relevant future work is proposed.

CHAPTER 2

EXACT SCATTERING SOLUTIONS

In this chapter, the exact eigenfunction series solution will be derived. Due to the azimuthal symmetry of cylinders, the calculation of the scattered field can be carried out using the modal approach. First, the total field is expanded into a series of cylindrical harmonics. By matching boundary conditions, the eigenfunction solution can be obtained exactly. Unfortunately, this series solution becomes slowly convergent at higher frequencies ($k_0 b > 10$). Using the Watson transformation, this slowly convergent series can be converted into a series more efficient to numerical computation. The series is then converted into a contour integral, which can then be solved using residue calculus. The final result is the residue series solution, which represents the sum of the resonant modes of the structure. The residue series solution is quickly convergent for high frequencies.

Eigenfunction Series Solution

Consider an infinite perfectly conducting cylinder of radius a whose axis lies along the z-axis lying in free space. The conducting cylinder is coated with material of permittivity ϵ_1 and permeability μ_1. The coating has a thickness d and thus extends from $\rho = a$ to $\rho = b$, where $b = a + d$. See Figure 2.1 for the TM case. We assume an incident plane wave whose $\overline{k}$-vector is perpendicular to the axis of the cylinder. Two incident polarizations, TM and TE, will be considered.

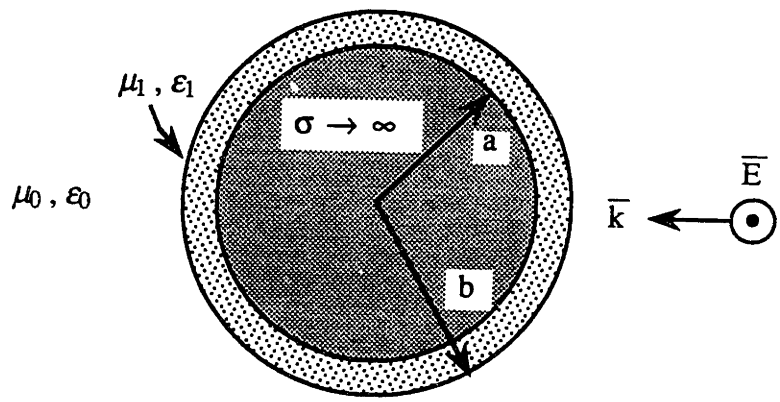

Figure 2.1 The Scattering Object: Coated Cylinder

The TM case

For the TM case, the electric field is parallel to the axis of the cylinder ($\hat{z}$-direction). Thus, the electric field is given by:

$$\overline{E}^i = \hat{z} E_0 e^{-ik_0 x} = \hat{z} E_0 e^{-ik_0 \rho \cos\phi} \tag{2.1}$$

where k_0 is the wavenumber in free space.

To match boundary conditions, the exponential is expressed as a sum of cylindrical harmonics that satisfies the Helmholtz wave equation:

$$e^{-ik_0 \rho \cos\phi} = \sum_{m=-\infty}^{\infty} a_m J_m(k_0 \rho) e^{im\phi}. \tag{2.2}$$

Taking advantage of orthogonality relations for $e^{im\phi}$ as well as the integral representation for the Bessel function

$$J_n(k_0\rho) = \frac{1}{2\pi}\int_0^{2\pi} d\phi e^{-ik_0\rho\cos\phi - in\phi + in\pi/2}, \tag{2.3}$$

we get $a_n = e^{-in\pi/2}$. Therefore,

$$e^{-ik_0\rho\cos\phi} = \sum_{n=-\infty}^{\infty} J_n(k_0\rho)e^{in\phi - in\pi/2} \tag{2.4}$$

and

$$\overline{E}^i = \hat{z}E_0 \sum_{n=-\infty}^{\infty} J_n(k_0\rho)e^{in(\phi-\pi/2)}. \tag{2.5}$$

The scattered waves can be expressed as a weighted sum of outgoing cylindrical harmonic waves:

$$\overline{E}^s = \hat{z}E_0 \sum_n A_n H_n^{(1)}(k_0\rho)e^{in(\phi-\pi/2)}. \tag{2.6}$$

We simply sum the incident and scattered fields to get the total field in the free space region:

$$\overline{E}_0 = \hat{z}E_0 \sum_n \left[J_n(k_0\rho) + A_n H_n^{(1)}(k_0\rho)\right] e^{in(\phi-\pi/2)} \tag{2.7}$$

while the total field in the coating is the superposition of outgoing and ingoing cylindrical waves.

$$\overline{E}_1 = \hat{z}E_0 \sum_n \left[B_n H_n^{(1)}(k_1\rho) + C_n H_n^{(2)}(k_1\rho)\right] e^{in(\phi-\pi/2)} \tag{2.8}$$

In each of the respective regions $(j = 0,1)$, the magnetic field can be derived from the electric field using Faraday's law:

$$\overline{H}_j = \frac{1}{i\omega\mu_j}\left[\hat{\rho}\frac{1}{\rho}\frac{\partial}{\partial\phi}E_{jz} - \hat{\phi}\frac{\partial}{\partial\rho}E_{jz}\right]. \tag{2.9}$$

Now that the formulations of total electric and magnetic fields have been obtained, we now apply boundary conditions. Setting tangential $\overline{E}$ and tangential $\overline{H}$ continuous at $\rho = b$ gives the relations:

$$B_n H_n^{(1)}(k_1 a) + C_n H_n^{(2)}(k_1 a) = J_n(k_0 b) + A_n H_n^{(1)}(k_0 b)$$
$$\frac{k_0}{\mu_0}\left[J_n'(k_0 b) + A_n H_n^{(1)\prime}(k_0 b)\right] = \frac{k_1}{\mu_1} B_n H_n^{(1)\prime}(k_1 b) + C_n H_n^{(2)\prime}(k_1 b)$$

Setting tangential $\overline{E}$ equal to zero at $\rho = R$ gives the following:

$$B_n H_n^{(1)}(k_1 a) + C_n H_n^{(2)}(k_1 a) = 0$$

After some algebraic manipulation, we get the result:

$$A_n^m = -\frac{J_n'(k_0 b) - S_n^m J_n(k_0 b)}{H_n^{(1)\prime}(k_0 b) - S_n^m H_n^{(1)}(k_0 b)} \tag{2.10}$$

where

$$S_n^m = \frac{\mu_0 k_1}{\mu_1 k}\frac{H_n^{(1)\prime}(k_1 b)H_n^{(2)}(k_1 a) - H_n^{(2)\prime}(k_1 b)H_n^{(1)}(k_1 a)}{H_n^{(1)}(k_1 b)H_n^{(2)}(k_1 a) - H_n^{(2)}(k_1 b)H_n^{(1)}(k_1 a)}. \tag{2.11}$$

This can also be equivalently expressed in terms of Bessel and Neumann functions:

$$S_n^m = \frac{Z_0}{Z_1}\frac{J_n(k_1 a)N_n'(k_1 b) - N_n(k_1 a)J_n'(k_1 b)}{J_n(k_1 a)N_n(k_1 b) - N_n(k_1 a)J_n(k_1 b)}. \tag{2.12}$$

where Z_0 and Z_1 are the impedances of free space and coating, respectively.

Since $J_n(\xi) = \frac{1}{2}[H_n^{(1)}(\xi) + H_n^{(2)}(\xi)]$, the field in the free space region can be expressed as:

$$\overline{E}_0 = \hat{z}\frac{1}{2}E_0 \sum_n \left[H_n^{(2)}(k_0\rho) - \frac{N_n^m}{D_n^m}H_n^{(1)}(k_0\rho)\right] e^{in(\phi-\pi/2)} \tag{2.13}$$

where

$$\begin{aligned} N_n^m =& \mu_1 k_0 H_n^{(2)\prime}(k_0 b)\left[H_n^{(1)}(k_1 b)H_n^{(2)}(k_1 a) - H_n^{(2)}(k_1 b)H_n^{(1)}(k_1 a)\right] \\ & - \mu_0 k_1 H_n^{(2)}(k_0 b)\left[H_n^{(1)\prime}(k_1 b)H_n^{(2)}(k_1 a) - H_n^{(2)\prime}(k_1 b)H_n^{(1)}(k_1 a)\right] \end{aligned} \tag{2.14}$$

$$\begin{aligned} D_n^m =& \mu_1 k_0 H_n^{(1)\prime}(k_0 b)\left[H_n^{(1)}(k_1 b)H_n^{(2)}(k_1 b) - H_n^{(2)}(k_1 b)H_n^{(1)}(k_1 a)\right] \\ & - \mu_0 k_1 H_n^{(1)}(k_0 b)\left[H_n^{(1)\prime}(k_1 b)H_n^{(2)}(k_1 a) - H_n^{(2)\prime}(k_1 b)H_n^{(1)}(k_1 a)\right]. \end{aligned} \tag{2.15}$$

N_n^m and D_n^m comprise the numerator and denominator, respectively, of the ratio A_n. The superscript m refers to values in the TM case. In later sections where the TE case is presented, the superscript e will be used.

The TE Case

For the TE case, the magnetic field is parallel to the axis of the cylinder ($\hat{z}$-direction). The magnetic field in the free space and coating is, respectively,

$$\overline{H}_0 = \hat{z}H_0 \sum_n \left[J_n(k_0\rho) + A_n H_n^{(1)}(k_0\rho)\right] e^{in(\phi-\pi/2)} \tag{2.16}$$

$$\overline{H}_1 = \hat{z}H_0 \sum_n \left[B_n H_n^{(1)}(k_1\rho) + C_n H_n^{(2)}(k_1\rho)\right] e^{in(\phi-\pi/2)} \tag{2.17}$$

The electric field in each respective region $(j = 0, 1)$ is obtained using Ampere's Law:

$$\overline{E}_j = -\frac{1}{i\omega\epsilon_j}\left[\hat{\rho}\frac{1}{\rho}\frac{\partial}{\partial\phi}H_{jz} - \phi\frac{\partial}{\partial\rho}H_{jz}\right] \tag{2.18}$$

Applying boundary conditions at $\rho = b$ and $\rho = R$ gives the relations:

$$\begin{aligned}
B_n H_n^{(1)}(k_1 a) + C_n H_n^{(2)}(k_1 a) &= J_n(k_0 b) + A_n H_n^{(1)}(k_0 b) \\
\frac{k_0}{\epsilon_0}\left[J_n'(k_0 b) + A_n H_n^{(1)\prime}(k_0 b)\right] &= \frac{k_1}{\epsilon_1} B_n H_n^{(1)\prime}(k_1 b) + C_n H_n^{(2)\prime}(k_1 b) \\
J_n'(k_1 a) + A_n H_n^{(1)\prime}(k_1 a) &= 0
\end{aligned}$$

After some algebraic manipulation, we get the result:

$$A_n^e = -\frac{J_n'(k_0 b) - S_n^e J_n(k_0 b)}{H_n^{(1)\prime}(k_0 b) - S_n^e H_n^{(1)}(k_0 b)} \tag{2.19}$$

where

$$S_n^e = \frac{\mu_0 k_1}{\mu_1 k}\frac{H_n^{(1)\prime}(k_1 b)H_n^{(2)\prime}(k_1 a) - H_n^{(2)\prime}(k_1 b)H_n^{(1)\prime}(k_1 a)}{H_n^{(1)}(k_1 b)H_n^{(2)\prime}(k_1 a) - H_n^{(2)}(k_1 b)H_n^{(1)\prime}(k_1 a)}. \tag{2.20}$$

This can also be equivalently expressed in terms of Bessel and Neumann functions:

$$S_n^e = \frac{Z_0}{Z_1}\frac{J_n'(k_1 a)N_n'(k_1 b) - N_n'(k_1 a)J_n'(k_1 b)}{J_n'(k_1 a)N_n(k_1 b) - N_n'(k_1 a)J_n(k_1 b)}. \tag{2.21}$$

The free space solution is:

$$\overline{H}_0 = \hat{z}\frac{1}{2}H_0\sum_n\left[H_n^{(2)}(k_0\rho) - \frac{N_n^e}{D_n^e}H_n^{(1)}(k_0\rho)\right]e^{in(\phi-\pi/2)} \tag{2.22}$$

where

$$N_n^e = \epsilon_1 k_0 H_n^{(2)\prime}(k_0 b)\left[H_n^{(1)}(k_0 b)H_n^{(2)\prime}(k_1 a) - H_n^{(2)}(k_1 b)H_n^{(1)\prime}(k_1 a)\right] - \epsilon k_1 H_n^{(2)}(k_0 b)\left[H_n^{(1)\prime}(k_1 b)H_n^{(2)\prime}(k_1 a) - H_n^{(2)\prime}(k_1 b)H_n^{(1)\prime}(k_1 a)\right] \quad (2.23)$$

$$D_n^e = \epsilon_1 k_0 H_n^{(1)\prime}(k_0 b)\left[H_n^{(1)}(k_1 b)H_n^{(2)\prime}(k_1 a) - H_n^{(2)}(k_1 b)H_n^{(1)\prime}(k_1 a)\right] - \epsilon k_1 H_n^{(1)}(k_0 b)\left[H_n^{(1)\prime}(k_1 b)H_n^{(2)\prime}(k_1 a) - H_n^{(2)\prime}(k_1 b)H_n^{(1)\prime}(k_1 a)\right]. \quad (2.24)$$

Integral Solution

When the radius of the cylinder is not small compared to wavelength $(k_0 b > 1)$, the series solution (2.11) converges very slowly, making it impractical for numerical computation. The Watson transformation relates this slowly convergent series to a contour integral as shown in Figure 2.2. According to Cauchy's theorem, the contour integral is equal to the sum of the residues. Assuming that A_ν has no poles on the real axis, the residue poles arise from the zeros of $\sin \nu\pi$ in the denominator. Thus we have the relation

$$\sum_{n=-\infty}^{\infty} e^{in\phi} A_n = \frac{i}{2}\oint_C d\nu \frac{e^{i\nu(\phi-\pi)}}{\sin \nu\pi} A_\nu, \quad (2.25)$$

To apply the Watson transformation, we let

$$A_\nu = \frac{1}{2}\left[H_\nu^{(2)}(k_0\rho) - \frac{N_\nu^m}{D_\nu^m} H_\nu^{(1)}(k_0\rho)\right] e^{-i\nu\pi/2} \quad (2.26)$$

such that the electric field is

$$\overline{E}_0 = \hat{z} E_0 \sum_n e^{in\phi} A_n = \hat{z} E_0 \frac{i}{2}\oint_C d\nu \frac{e^{i\nu(\phi-\pi)}}{\sin \nu\pi} A_\nu$$

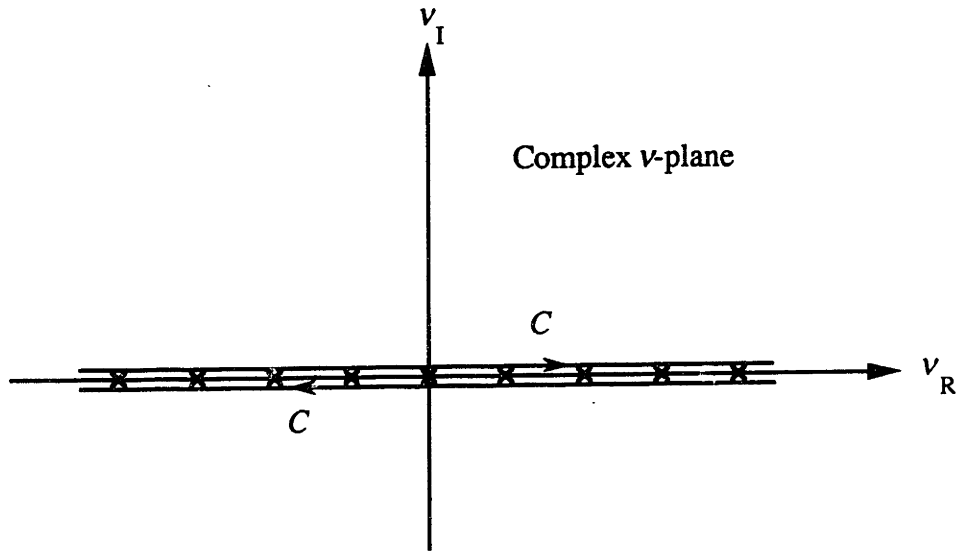

Figure 2.2 Contour for Watson Transformation with poles

$$= E_0 \lim_{\delta \to 0} \frac{i}{2} \left[\int_{-\infty+i\delta}^{\infty+i\delta} + \int_{\infty-i\delta}^{-\infty-i\delta} \right] d\nu \frac{e^{i\nu(\phi-\pi)}}{\sin \nu\pi} A_\nu$$

$$= E_0 \frac{i}{2} \int_{-\infty}^{\infty} \frac{1}{\sin \nu\pi} \left[e^{i\nu(\phi-\pi)} A_\nu + e^{-i\nu(\phi-\pi)} A_{-\nu} \right]. \tag{2.27}$$

Since

$$H_{-\nu}^{(1)}(\xi) = e^{i\nu\pi} H_\nu^{(1)}(\xi)$$

$$H_{-\nu}^{(2)}(\xi) = e^{-i\nu\pi} H_\nu^{(2)}(\xi),$$

it can be easily shown that

$$D_{-\nu}^m(\xi) = e^{i\nu\pi} D_\nu^m(\xi)$$

$$N_{-\nu}^m(\xi) = e^{-i\nu\pi} N_\nu^m(\xi).$$

Therefore,

$$A_{-\nu}(\xi) = e^{-i\nu\pi} A_{\nu}(\xi).$$

Finally, the solution can be simplified as

$$\overline{E}_0 = \hat{z} E_0 \frac{i}{2} \int_{-\infty}^{\infty} d\nu \frac{\cos\nu(\phi-\pi)}{\sin\nu\pi} \left[H_{\nu}^{(2)}(k_0\rho) - \frac{N_{\nu}^{m}}{D_{\nu}^{m}} H_{\nu}^{(1)}(k_0\rho) \right] e^{-i\nu\pi/2}. \tag{2.28}$$

Similarly, for the TE case, the Watson Transformation yields the following $\overline{H}$-field:

$$\overline{H}_0 = \hat{z} H_0 \frac{i}{2} \int_{-\infty}^{\infty} d\nu \frac{\cos\nu(\phi-\pi)}{\sin\nu\pi} \left[H_{\nu}^{(2)}(k_0\rho) - \frac{N_{\nu}^{e}}{D_{\nu}^{e}} H_{\nu}^{(1)}(k_0\rho) \right] e^{-i\nu\pi/2}. \tag{2.29}$$

Residue Series Solution

The solution for the fields in the TM case (2.28) and the TE case (2.29) can be solved by deforming the contour into a closed loop in the upper-half plane as shown in Figure 2.3. The integral around the half-circle contour goes to zero as R approaches infinity in the ν-plane. By Cauchy's theorem, the integrals in (2.28) and (2.29) are equal to the sum of the residues of the poles of the integrand in the upper-half ν-plane. Since the $H_{\nu}^{(1)}(k_0\rho)$ and $H_{\nu}^{(2)}(k_0\rho)$ terms in (2.28) and (2.29) has no poles in the upper ν-plane, the residues are picked at the poles of the ratio $\frac{N_{\nu}}{D_{\nu}}$. More simply, the pole locations are chosen at the zeros of D_{ν}.

Therefore, solutions for both TM and TE take the form:

$$\overline{F} = \hat{z}\pi F_0 \sum_{n=1}^{\infty} \frac{N_{\nu_n}}{[\frac{\partial}{\partial\nu} D_{\nu}]_{\nu=\nu_n}} \frac{\cos\nu_n(\phi-\pi)}{\sin\nu_n\pi} e^{-i\nu_n\pi/2} H_{\nu_n}^{(1)}(k_0\rho) \tag{2.30}$$

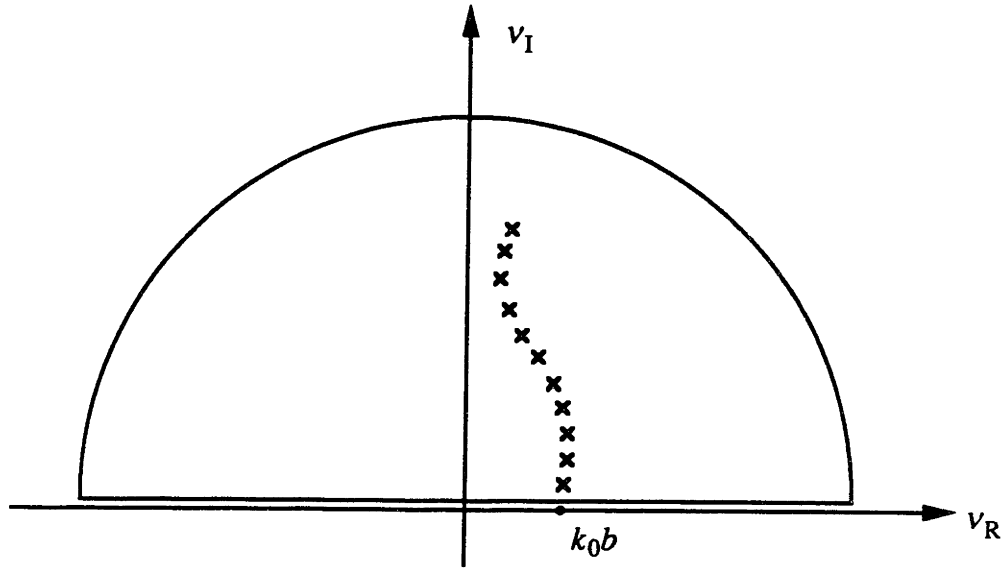

Figure 2.3 The Upper Half Plane Contour and Poles of the Modal Expansion

where $\overline{F}$ is the electric field for the TM case and magnetic field for the TE case. ν_n is defined as the n^{th} root of the modal equation

$$D_\nu = 0. \tag{2.31}$$

Equation (2.30) is the residue series solution, while (2.31) is the modal equation whose solution defines the values of ν_n. ν_n refers to the root of (2.31) with the n^{th} lowest imaginary part. Each term of the summation in (2.30) represents a natural mode excited within the structure. Via the residue series solution, the total scattered field is generated by a series of scattering contributions of each resonant mode. Every mode or term in the residue series corresponds to a unique propagation constant ν_n and amplitude. The propagation constant is determined as the solution to the tran-

scendental equation $D_\nu = 0$ (2.31). Its real part equals the phase velocity of the waves of the excited modes; its imaginary part equals the attenuation of the waves.

$$\nu' = v_p \tag{2.32}$$

$$\nu'' = \alpha \tag{2.33}$$

where

$$\nu = \nu' + i\nu'' \tag{2.34}$$

Once equation (2.31) is solved and ν_n is obtained, the amplitude is calculated by plugging ν_n into the expression within the summation of (2.30).

Numerical Computation

Of the three exact solutions, the eigenfunction series and residue series solutions are easy to implement numerically because they are summations instead of integrals. In the low frequency limit, when $k_0 b \ll 20$, the eigenfunction series solution will converge quickly and thus yield accurate results. For high frequencies ($k_0 b > 20$), where the eigenfunction solution becomes slowly convergent, the residue series solution is very quickly convergent. Usually only the first two terms of the residue series are necessary for high accuracy. While the eigenfunction solution gives scattering for all angles $0 < \phi < 2\pi$, the residue series solution is convergent only in the deep shadow region. This is due to the fact that

$$\frac{\cos \nu_n(\phi - \pi)e^{-i\nu_n \pi/2}}{\sin \nu_n \pi} = \frac{-i[e^{i\nu_n(\phi - \pi/2)} + e^{i\nu_n(3\pi/2 - \phi)}]}{1 - e^{i\nu_n 2\pi}}. \tag{2.35}$$

Using the Debye approximation for Hankel functions,

$$H_{\nu_n}^{(1)}(k_0\rho) \approx \sqrt{\frac{2}{\pi(k_0^2\rho^2-\nu_n^2)^{1/2}}}e^{i(\sqrt{k_0^2\rho^2-\nu_n^2}-\nu_n\cos^{-1}(\nu_n/k_0\rho)-\pi/4)} \tag{2.36}$$

Since we may approximate $\nu_n \approx k_0 b$ for the first few dominant terms, the exponential dependence is approximately equal to:

$$e^{ik_0\sqrt{\rho^2-b^2}}\{e^{i\nu_n[\phi-(\pi/2)-\cos^{-1}(b/\rho)]}+e^{i\nu_n[3\pi/2-\phi-\cos^{-1}(b/\rho)]}\} \tag{2.37}$$

Since the imaginary part of ν_n is positive, equation (2.37) shows that the residue series will converge only when

$$\frac{\pi}{2}+\cos^{-1}\left(\frac{b}{\rho}\right) < \phi < \frac{3\pi}{2}-\cos^{-1}\left(\frac{b}{\rho}\right). \tag{2.38}$$

This region is the shadow region.

A high frequency solution for the illuminated region is obtained by evaluating the integral solutions (2.28) and (2.29). These integrals are solved in the following chapter.

CHAPTER 3

SPECULAR FIELD

In Chapter 2, an exact eigenfunction series solution was derived by matching boundary conditions. Because the eigenfunction solution is slowly convergent for higher frequencies, the Watson Transformation is used to convert it into another exact solution more suitable for higher frequency computation. Nevertheless, the computation of the exact solutions (2.28-2.30) presents difficulties because they are not in closed form as are the eigenfunction solutions (2.13) and (2.22).

This chapter presents the derivation of an approximate solution to equations (2.28) and (2.29) by Kim and Wang [16]. These solutions will give the specular scattered field as viewed by an observer in the illuminated region. The specular field yields the greatest contribution to scattering in the illuminated region.

Equations (2.28) and (2.29) both can be generalized into the format:

$$\overline{F}_0 = \hat{z} F_0 \frac{i}{2} \int_{-\infty}^{\infty} d\nu \frac{\cos \nu(\phi - \pi)}{\sin \nu\pi} \left[H_\nu^{(2)}(k_0\rho) - \frac{N_\nu}{D_\nu} H_\nu^{(1)}(k_0\rho) \right] e^{-i\nu\pi/2} \tag{3.1}$$

where $\overline{F}_0$ is the free space electric field for the TM case and magnetic field for the TE case.

Since

$$\frac{\cos \nu(\phi - \pi)}{\sin \nu\pi} = -ie^{i\nu\phi} + e^{i\nu\pi} \frac{\cos \nu\phi}{\sin \nu\pi} \tag{3.2}$$

(3.1) can be broken into two parts:

$$\overline{F}_0 = \overline{F}^{dom} + \overline{F}^{cw} \tag{3.3}$$

where

$$\overline{F}^{dom} = \hat{z}F_0\frac{1}{2}\int_{-\infty}^{\infty} d\nu e^{i\nu\phi}\left[H_\nu^{(2)}(k\rho) - \frac{N_\nu}{D_\nu}H_\nu^{(1)}(k\rho)\right]e^{-i\nu\pi/2} \tag{3.4}$$

and

$$\overline{F}^{cw} = \hat{z}F_0\frac{1}{2}\int_{-\infty}^{\infty} d\nu\frac{\cos\nu\phi}{\sin\nu\pi}\left[H_\nu^{(2)}(k\rho) - \frac{N_\nu}{D_\nu}H_\nu^{(1)}(k\rho)\right]e^{i\nu\pi/2}. \tag{3.5}$$

$\overline{F}^{dom}$ is the field due to the sum total of incident field, reflections, and dominant diffraction effects. $\overline{F}^{cw}$ is due to the multiply encircling creeping waves.

To calculate the specular reflections, we need to break up (3.4) into two parts:

$$F^{dom} = I_1 + I_2 \tag{3.6}$$

where

$$I_1 = \frac{1}{2}F_0\int_{-\infty}^{\infty} d\nu e^{i\nu\phi}H_\nu^{(2)}(k_0\rho)e^{-i\nu\pi/2} \tag{3.7}$$

and

$$I_2 = -\frac{1}{2}F_0\int_{-\infty}^{\infty} d\nu e^{i\nu\phi}\frac{N_\nu}{D_\nu}H_\nu^{(1)}(k_0\rho)e^{-i\nu\pi/2} \tag{3.8}$$

Solving I_1

By replacing the Hankel function in (3.7) with its integral representation

$$H_\nu^{(2)}(k_0\rho) = \frac{1}{\pi}\int_{\Gamma_2} d\alpha e^{i(k_0\rho\cos\alpha+\nu\alpha-\nu\pi/2)} \tag{3.9}$$

and switching integrals, I_1 becomes

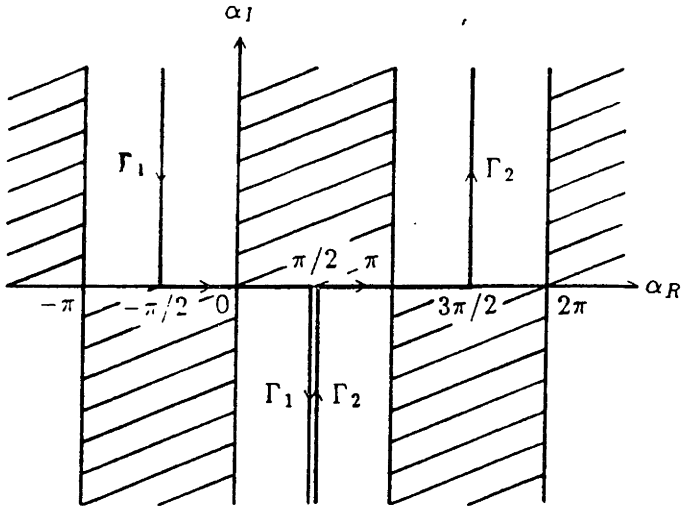

Figure 3.1 Contour Path for Hankel Functions of First and Second Kind

$$I_1 = \frac{1}{2\pi} F_0 \int_{\Gamma_2} d\alpha e^{ik_0\rho\cos\alpha} \int_{-\infty}^{\infty} d\nu e^{-i\nu(\phi+\pi-\alpha)} \tag{3.10}$$

The integration path Γ_2 for the integral representation of $H_\nu^{(2)}(k_0\rho)$ is shown in Figure 3.1.

The inverse Fourier transform of a complex exponential is a delta function. Thus, I_1 simplifies into:

$$\begin{aligned} I_1 &= \frac{1}{2\pi} \int_{\Gamma_2} d\alpha e^{ik_0\rho\cos\alpha} 2\pi\delta(\alpha - \phi - \pi) \\ &= F_0 e^{-ik_0\rho\cos\phi} \end{aligned} \tag{3.11}$$

We assumed that $\alpha = \phi + \pi$ lies on the contour Γ_2 to arrive at the final expression in

(3.9). This implies that

$$-\frac{\pi}{2} \leq \phi \leq \frac{\pi}{2} \tag{3.12}$$

Therefore, under constraints imposed by (3.10), I_1 is simply an expression for the incident field.

Solving I_2

I_2 will be solved asymptotically using the stationary phase approximation. Solving I_2 is more difficult than I_1 because the former contains the expression $\frac{N_\nu}{D_\nu}$, which contains Hankel functions having four different arguments $(k_0\rho,\ k_0b,\ k_1a,\ k_1b)$. This difficulty can be handled by dividing (3.8) into two parts:

$$I_2 = F_{2>} + F_{2<} \tag{3.13}$$

where

$$F_{2>} = -\frac{1}{2}\int_{k_0b}^{\infty} d\nu \frac{N_\nu}{D_\nu} H_\nu^{(1)}(k_0\rho) e^{i\nu(\phi-\pi/2)} \tag{3.14}$$

and

$$F_{2<} = -\frac{1}{2}\int_{-\infty}^{k_0b} d\nu \frac{N_\nu}{D_\nu} H_\nu^{(1)}(k_0\rho) e^{i\nu(\phi-\pi/2)} \tag{3.15}.$$

The stationary phase approximation states that most of the contribution to the integral comes from the saddle point. If we assume that the stationary phase point ν_s is not close to k_0b, then the contribution due to the end point $\nu = k_0b$ is negligible. Assuming that ν is not close to k_0b such that $\nu - k_0b/gg|\nu|^{\frac{1}{3}}$, then

$$H_\nu^{(1)}(k_0b) \approx -H_\nu^{(2)}(k_0b) \tag{3.16}.$$

With the approximation (3.16), $\frac{N_\nu}{D_\nu}$ can be simplified as:

$$\left(\frac{N_\nu}{D_\nu}\right)^{m,e} \approx -1 \tag{3.17}$$

$F_{2>}$, in turn, simplifies into:

$$F_{2>} = -\frac{1}{2}\int_{k_0 b}^{\infty} d\nu e^{i\nu\phi} H_\nu^{(1)}(k_0\rho) e^{-i\nu\pi/2} \tag{3.18}$$

(3.18) holds true for both the TE and TM cases.

The far-field region implies that $\rho \gg b$ and therefore $\nu \ll k_0 b$. So in the far-field, the Hankel function in (3.16) can be replaced by the first term of Debye's asymptotic approximation.

$$H_\nu^{(1)}(k_0\rho) \approx \sqrt{\frac{2}{\pi k_0 \rho \sin\alpha}} e^{-i\pi/4} e^{ik_0\rho(\sin\alpha - \alpha\cos\alpha)} \tag{3.19}$$

where

$$\cos\alpha = \frac{\nu}{k_0\rho} \tag{3.20}$$

under the constraint that the real part of α is between 0 and π.

$$0 < \Re\{\alpha\} < \pi \tag{3.21}$$

$F_{2>}$ can be rewritten as:

$$F_{2>} = -F_0 \frac{e^{-i\pi/4}}{\sqrt{2\pi k_0\rho}} \int_{k_0 b}^{\infty} d\nu \frac{e^{ik_0\rho\Psi(\nu)}}{\sqrt{\sin\alpha}} \tag{3.22}$$

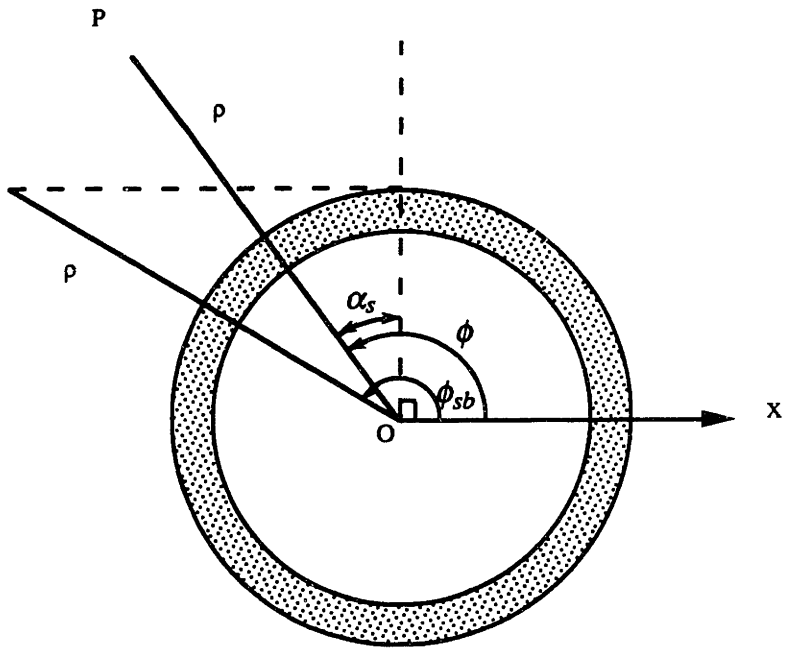

Figure 3.2 The physical meaning of the stationary point

such that

$$\Phi(\nu) = \sin\alpha - \frac{\nu}{k_0\rho}(\alpha - \phi + \pi/2) \tag{3.23}$$

The integral of (3.22) can be deformed into the steepest descent path Γ_{sd}. Then it can be evaluated at the stationary phase point ν_s:

$$F_{2>} = F_0 e^{-ik_0\rho\cos\phi} \tag{3.24}$$

under the constraint that $\Phi'(\nu_s) = 0$. Thus,

$$\alpha_s = \phi - \frac{\pi}{2}. \tag{3.25}$$

The physical meaning of α at the stationary point is shown in Figure 3.2.

Since α_s must lie on Γ_{sd} and satisfy (3.21), then we have the constraint on ϕ:

$$\frac{\pi}{2} \leq |\phi| < \phi_{sb} \tag{3.26}$$

where

$$\phi_{sb} = cos^{-1}\left(\frac{b}{\rho}\right) + \frac{\pi}{2}. \tag{3.27}$$

ϕ_{sb} is the angle of the shadow boundary, as shown in Figure 3.2.

Equations (3.11) and (3.24) are expression for the incident field. The former represents the incident field within the range $|\phi| \leq \frac{\pi}{2}$, the latter within $\frac{\pi}{2} \leq |\phi| \leq \phi_{sb}$. These two regions cover the entire illuminated region.

Solving $F_{2<}$

The stationary phase approximation is also applied to the evaluation of $F_{2<}$ of (3.15). First the variable $\frac{N_\nu}{D_\nu}$ is expressed in terms of Hankel functions, which are then replaced with their Debye approximations. Then the integral is evaluated at the stationary phase point.

$\frac{N_\nu}{D_\nu}$ in (3.13) can be expressed in terms of Hankel functions:

$$\left(\frac{N_\nu}{D_\nu}\right)^{m,e} = \frac{H_\nu^{(2)}(k_0 b)}{H_\nu^{(1)}(k_0 b)}\, C^{m,e} \tag{3.28}$$

where

$$C_\nu^{m,e} \equiv -\frac{H_\nu^{(2)'}(k_0 b)/H_\nu^{(2)}(k_0 b) + iS^{m,e}}{H_\nu^{(1)'}(k_0 b)/H_\nu^{(1)}(k_0 b) + iS^{m,e}} \tag{3.29}$$

$S_\nu^{m,e}$ is defined in equation (2.11) after replacing complex ν with integer n.

Because the integral over ν in (3.15) ranges from $-\infty$ to $k_0 b$, each Hankel functions in (3.28) and (3.29) can be replaced by its Debye approximations. The approximation for $H_\nu^{(1)}(k_0 b)$ is given in equation (3.19). The approximation for $H_\nu^{(2)}(k_0 b)$ is obtained by simply substituting i for $-i$ in (3.19). After the following substitutions, $\frac{N_\nu}{D_\nu}$ and C_ν can be approximated as:

$$\left(\frac{N_\nu}{D_\nu}\right)^{m,e} \approx ie^{-i2(k_0 b \sin\gamma - \gamma\nu)} \cdot C^{m,e} \tag{3.30}$$

where

$$C_\nu^{m,e} \approx \frac{\sin\gamma - S_\nu^{m,e}}{\sin\gamma + S_\nu^{m,e}} \tag{3.31}$$

and

$$\gamma = \cos^{-1}\left(\frac{\nu}{k_0 b}\right) \tag{3.32}$$

Substituting (3.30) into the integral expression of (3.15) yields:

$$F_{2<} = -\frac{1}{2}F_0 \int_{-\infty}^{k_0 b} d\nu i e^{-i2(k_0 b \sin\gamma - \gamma\nu)} \cdot C^{m,e} H_\nu^{(1)}(k_0\rho) e^{i\nu(\phi - \pi/2)}. \tag{3.33}$$

Replacing the Hankel function in (3.33) with the Debye approximation (3.19) gives the following result:

$$F_{2<} = -\frac{ie^{-i\pi/4}}{\sqrt{2\pi k_0\rho}} \int_{-\infty}^{k_0 b} d\nu \frac{C_\nu^{m,e}}{\sqrt{\sin\alpha}} e^{ik_0\rho\Phi(\nu)} \tag{3.34}$$

where

$$\Phi(\nu) \equiv \sin\alpha - \alpha\cos\alpha - 2\frac{b}{\rho}\sin\gamma + \frac{\nu}{k_0\rho}(2\gamma + \phi - \pi/2) \tag{3.35}$$

To find derivatives of Φ, we use the relations:

$$\frac{d\alpha}{d\nu} = \frac{-1}{k_0 \rho \sin\alpha}$$

and

$$\frac{d\gamma}{d\nu} = \frac{-1}{k_0 b \sin\gamma}$$

Taking derivatives of Φ with respect to ν gives:

$$\Phi'(\nu) = \frac{1}{k_0\rho}(-\alpha + 2\gamma + \phi - \pi/2) \tag{3.36}$$

and

$$\Phi''(\nu) = \frac{1}{k_0^2\rho}\left(\frac{2}{k_0\rho\sin\gamma} - \frac{1}{k_0 b \sin\alpha}\right) \tag{3.37}$$

At the stationary phase point $\nu = \nu_s$, $\Phi'(\nu_s) = 0$. This determines the relationship

$$\alpha_s - 2\gamma_s = \phi - \pi/2 \tag{3.38}$$

where

$$\alpha_s = \cos^{-1}\left(\frac{\nu_s}{k_0\rho}\right) \tag{3.39}$$

$$\gamma_s = \cos^{-1}\left(\frac{\nu_s}{k_0 b}\right). \tag{3.40}$$

Thus, at the stationary phase point ν_s,

$$\Phi(\nu_s) = \sin\alpha_s - \frac{2b}{\rho}\sin\gamma_s \tag{3.41}$$

and

$$\Phi''(\nu_s) = \frac{1}{k_0^2 \rho}\left(\frac{1}{\rho \sin\alpha_s} - \frac{2}{b \sin\gamma_s}\right). \tag{3.42}$$

The physical meaning of the stationary phase point is shown in Figure 3.3. The stationary points can be expressed in terms of the geometric quantities as shown in Figure 3.3.

$$l_s = \rho \sin\alpha_s - b \sin\gamma_s \tag{3.43}$$

$$\gamma_s = \pi/2 - \theta_i = \pi/2 - \phi_i \tag{3.44}$$

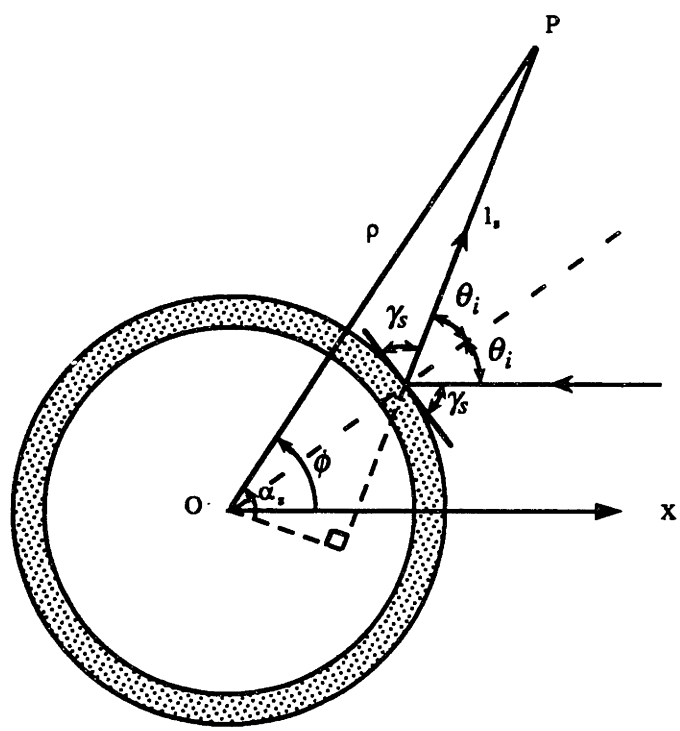

Figure 3.3 The physical meaning of the stationary point

The values of α_s and γ_s at the stationary phase point fall under the constraints:

$$0 \leq \Re\{\alpha_s\} \leq \pi$$

$$0 \leq \Re\{\gamma_s\} \leq \pi \tag{3.45}$$

The integral of (3.34) can now be evaluated using the stationary phase values of $\Phi(\nu)$ and its derivatives. Therefore,

$$F_{2<} = F_0 \frac{C_{\nu_s}}{\sqrt{\rho \sin \alpha_s}} e^{ik_0(\rho \sin \alpha_s - 2b \sin \gamma_s)} \sqrt{\frac{1}{\Phi''(\nu_s)}} \tag{3.46}$$

Finally, after some algebraic manipulation, the scattered field can be expressed as:

$$F_{2<} = F_0 C_{\nu_s} \sqrt{\frac{b \sin \gamma}{\rho \sin \alpha_s + l_s}} e^{ik_0 l_s} e^{-ik_0 b \sin \gamma_s} \tag{3.47}$$

Reflected Field

The final result for $F_{2<}$ can be represented as the field due to the specular reflection of the incident field. Thus, a solution of equation (3.47) can be cast into the Geometrical Theory of Diffraction (GTD) format. It becomes clear that this field solution consists of the reflected field when expressed in the form:

$$F_{2<} = u^i \cdot R^{m,e} \cdot S_p \cdot e^{ik_0 l_s} \tag{3.48}$$

where

$$S_p = \sqrt{\frac{b \sin \gamma}{\rho \sin \alpha_s + l_s}} \tag{3.52}$$

$u^i = F_0 e^{-ik_0 \rho \cos \phi_i}$ represents the incident ray impinging on point Q of the cylinder. $R^{m,e} = C^{m,e}$ is the reflection coefficient, S_p is the "spread factor", and $e^{ik_0 l_s}$ is the phase shift due to propagation. S_p represents the effect of the "spreading" of the power due to the curvature of the cylinder.

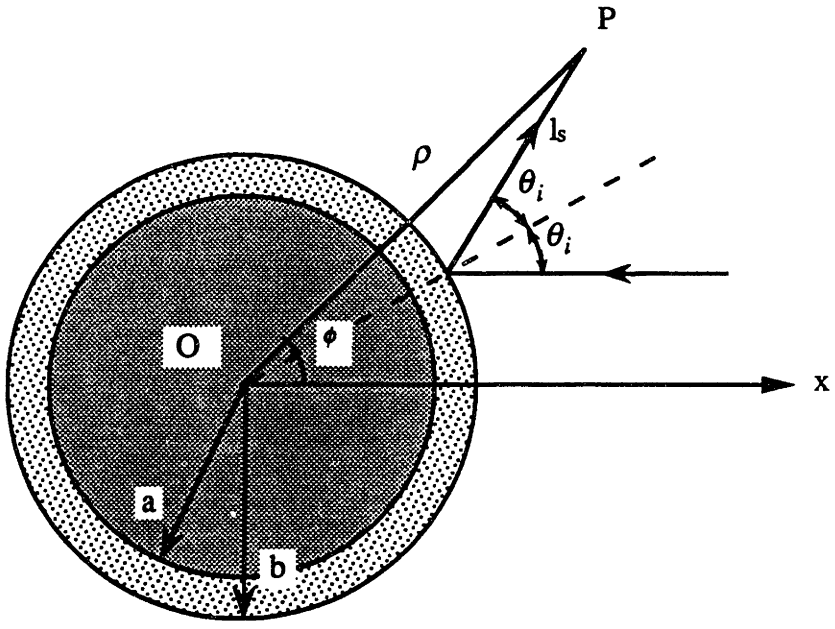

Figure 3.4 The Reflected Field

We can see that the reflection coefficient approximates to:

$$R^{m,e} \approx \frac{\cos \theta_i - S_\nu^{m,e}}{\cos \theta_i + S_\nu^{m,e}} \tag{3.53}$$

where $S_\nu^{m,e}$ is shown in equation (2.11).

Replacing the Hankel functions in $S^{m,e}$ by their Debye approximations yields the results for reflection coefficients for TM and TE, respectively.

$$R^e = -\frac{\eta_0 + i\eta_1 \cos\theta_i / \cos\theta_t \tan(\Psi)}{\eta_0 - i\eta_1 \cos\theta_i / \cos\theta_t \tan(\Psi)} \tag{3.54}$$

$$R^m = -\frac{\eta_0 + i\eta_1 \cos\theta_t / \cos\theta_i \tan(\Psi)}{\eta_0 - i\eta_1 \cos\theta_t / \cos\theta_i \tan(\Psi)} \tag{3.55}$$

where η_0 and η_1 are the characteristic impedances of the air and coating respectively. Ψ is defined as:

$$\Psi = k_1(b\sin\alpha_b - a\sin\alpha_a) - k_0 b(\alpha_b - \alpha_a)\sin\theta_i \tag{3.56}$$

where

$$\sin\alpha_b \equiv \cos\theta_t = \sqrt{1 - \left(\frac{k_0}{k_1}\sin\theta_i\right)^2} \tag{3.57}$$

and

$$\sin\alpha_a = \sqrt{1 - \left(\frac{b}{a}\sin\theta_t\right)^2} = \sqrt{1 - \left(\frac{k_0 b}{k_1 a}\sin\theta_i\right)^2} \tag{3.58}$$

From figure 3.3, applying the law of sines yields the relation between θ_i and ϕ:

$$\phi = 2\theta_i - \sin^{-1}\left[\frac{b}{\rho}\sin\theta_i\right]. \tag{3.59}$$

l_s can also be expressed in terms of ϕ and θ_i:

$$l_s = \frac{\rho\sin(\phi - \theta_i)}{\sin\theta_i} \tag{3.60}$$

Calculated Results

Programs were written that calculate the scattered field from cylinders using both the eigenfunction series solution and the GTD specular solution. The computer code employing the eigenfunction series are listed in Appendix A. The code using the GTD specular solution presented in this chapter are shown in Appendix B. Both programs have the same main program but have different subroutines linked to EIGEN.FOR.

To confirm the validity of the GTD specular solution, test cases are presented in Figures 3.5 to 3.10 to compare the results from the GTD specular and eigenfunction solutions. The incident field has unit amplitude, and the total fields a fixed radial distance are plotted. The parameters b, a, φ, and ρ are defined in Figures 3.1 and 3.4. ρ is the distance between the observation point P and the cylinder axis O. d is the coating thickness, $b-a$. The frequency such that $k_0 b = 20$ was chosen as an intermediary region such that the eigenfunction series, integral solution, and residue series all converge properly for comparison. This makes $b = 10/\pi\lambda \approx 3.18\lambda$. From equation (3.25), the shadow boundary lies at $\phi_{sb} \approx 161^o$.

While the eigenfunction series converges for all values of ϕ, the GTD solution converges only within the illuminated region $|\phi| < \phi_{sb}$. Thus all the plots show the eigenfunction results for total field from $\phi = 0^o$ to $\phi = 180^o$, but the GTD specular field only from $\phi = 0^o$ to $\phi_{sb} = 161^o$. As ϕ approaches ϕ_{sb}, the GTD solution gradually diverges from results of the eigenfunction solution.

As can be seen in nearly all the following figures, the GTD specular solution matches well with the eigenfunction solution deep in the lit region. Toward the shadow boundary, however, the GTD solution converges more slowly and loses accuracy. In

Figures 3.5 and 3.10, the large lobes of the eigenfunction curve in the shadow region indicates the existence of strong creeping wave diffraction at their own coating thicknesses. Strong creeping waves are due to a guidance phenomena of the coating. When the frequency and coating properties are such that guidance occurs, the cylinder is said to be resonant. In Figure 3.10 in particular, the GTD solution does not match so well with the eigenfunction solution. The large lobes in the shadow region indicated very strong creeping waves. In this case, the creeping waves are strong enough to significantly affect the scattered field even in the illuminated region. The smaller diffraction in the shadow region in Figures 3.6 to 3.9 indicate that the cylinder is not resonant for those cases.

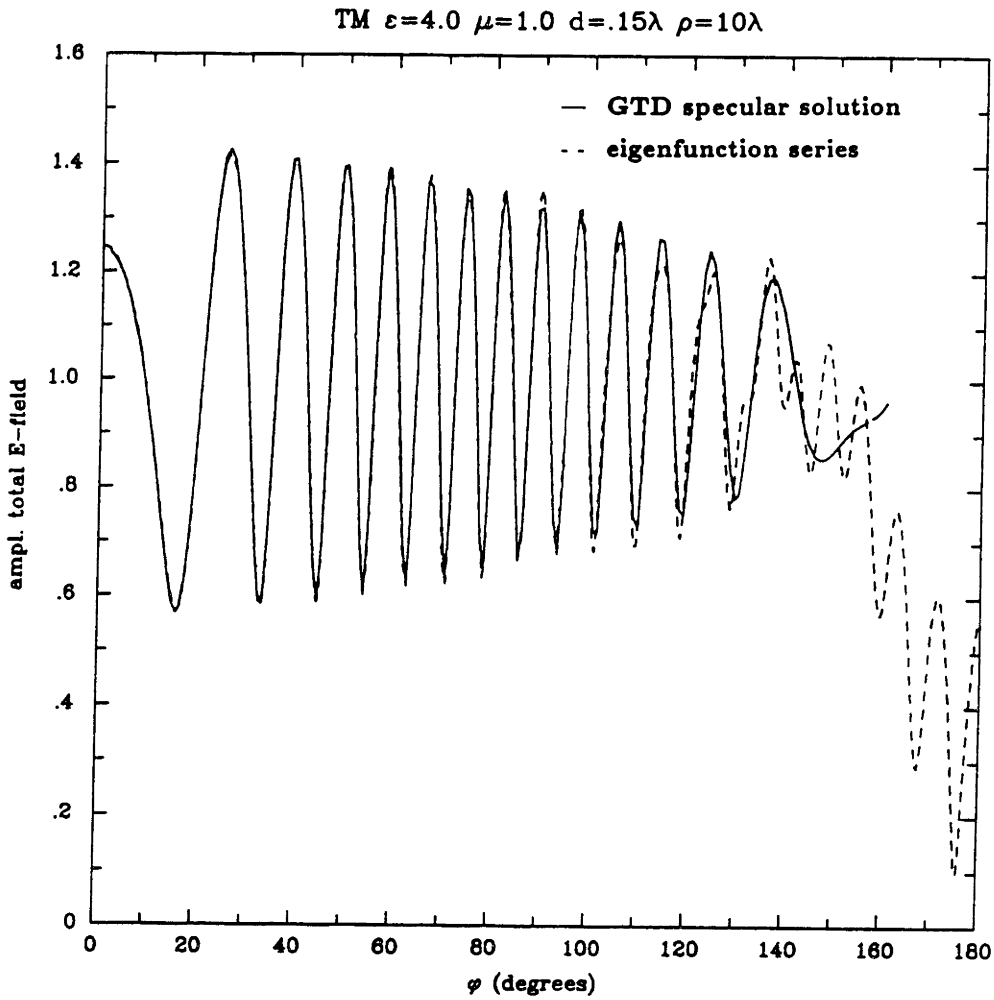

Figure 3.5 Comparison of GTD and eigenfunction solutions–TM

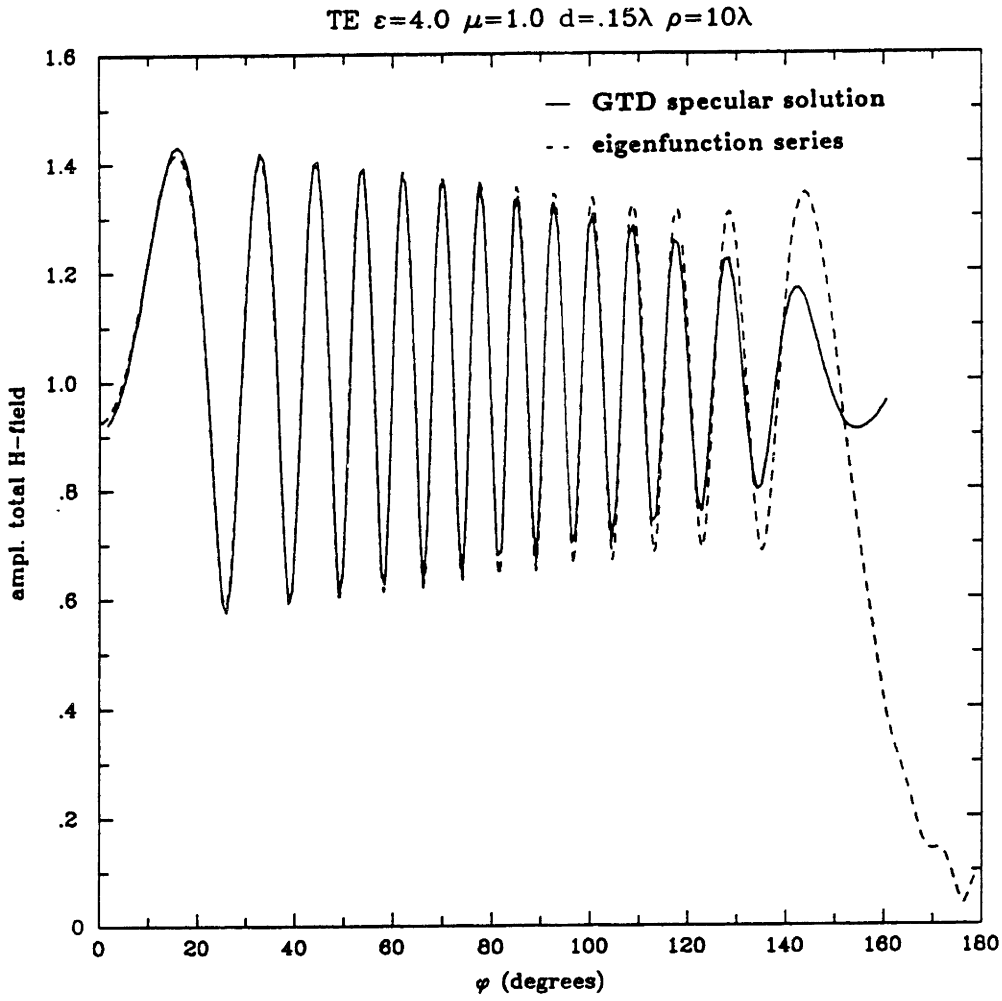

Figure 3.6 Comparison of GTD and eigenfunction solutions–TE

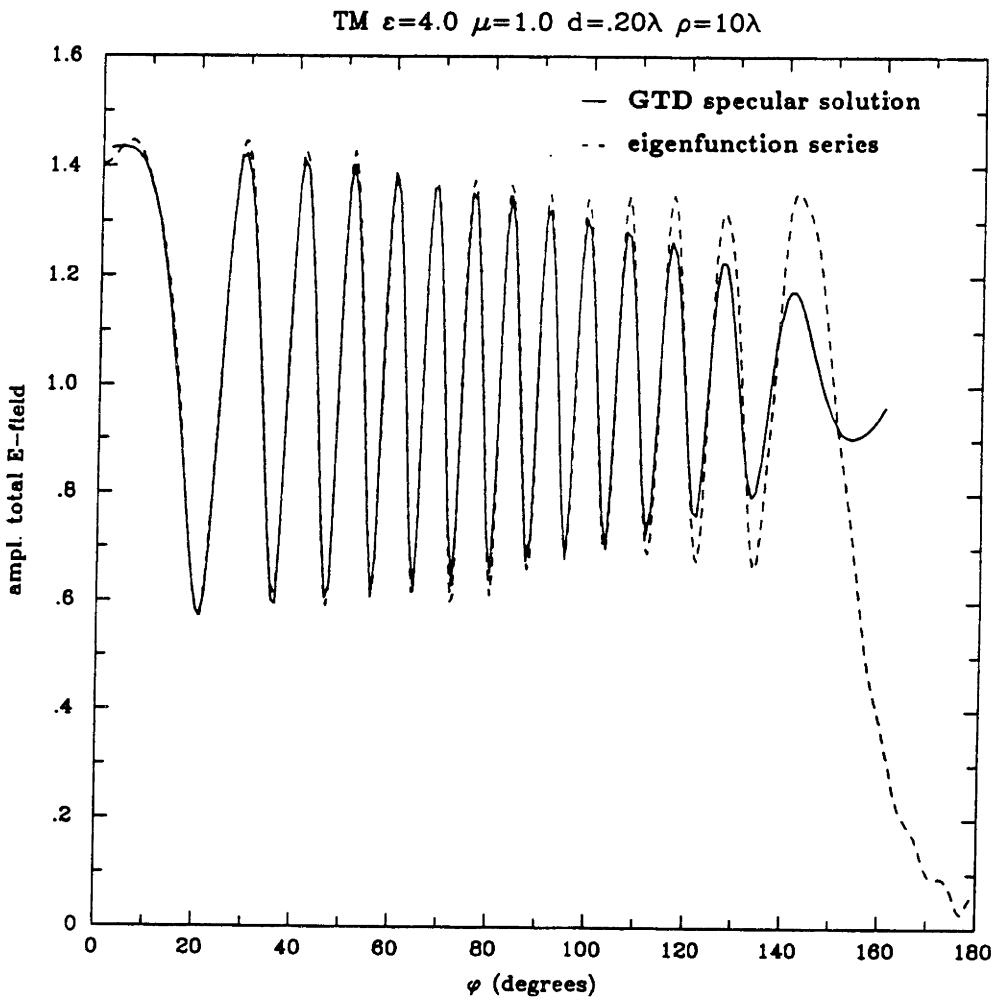

Figure 3.7 Comparison of GTD and eigenfunction solutions–TM

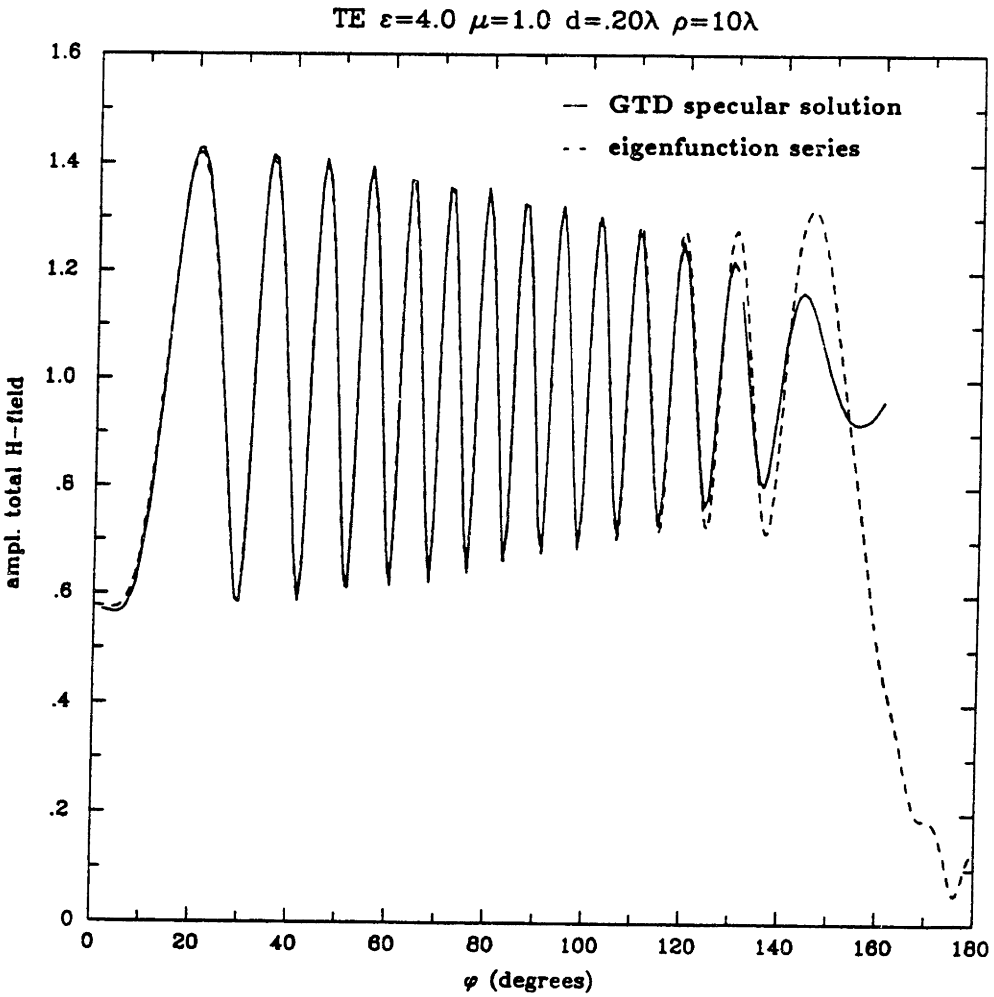

Figure 3.8 Comparison of GTD and eigenfunction solutions–TE

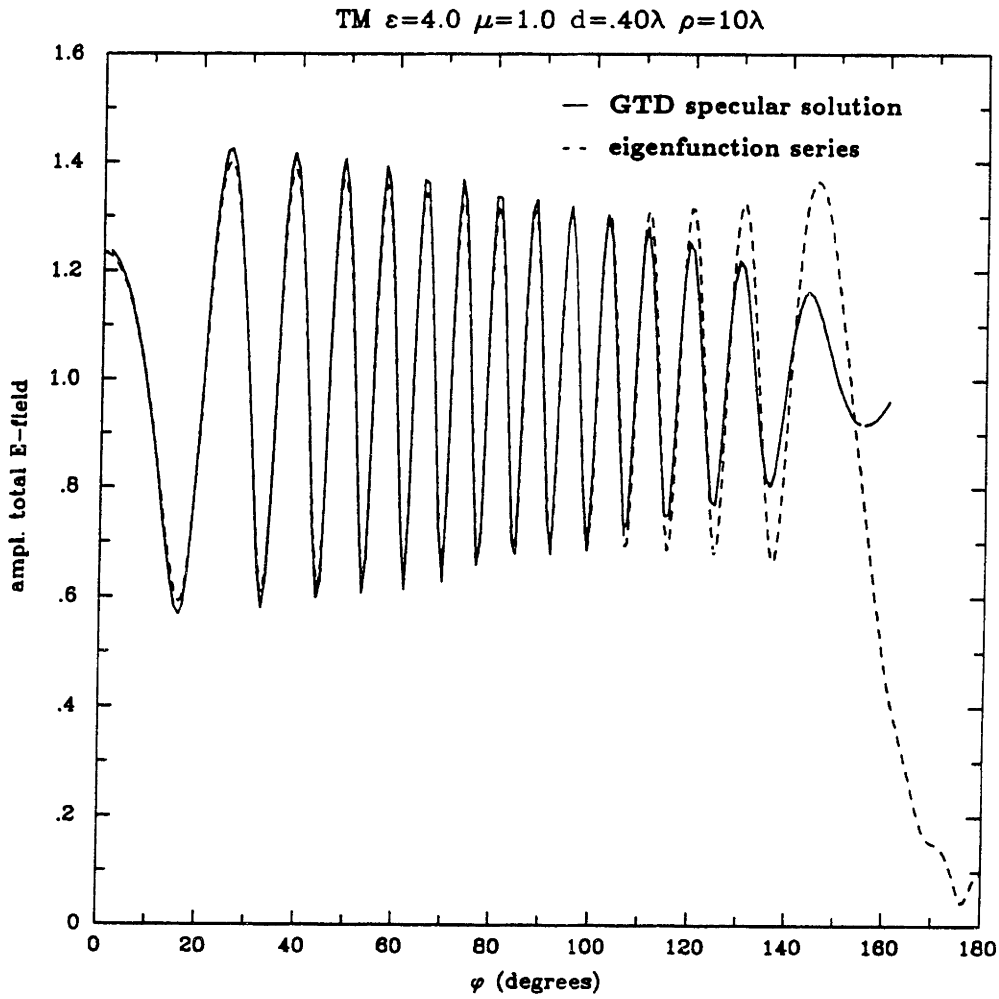

Figure 3.9 Comparison of GTD and eigenfunction solutions–TM

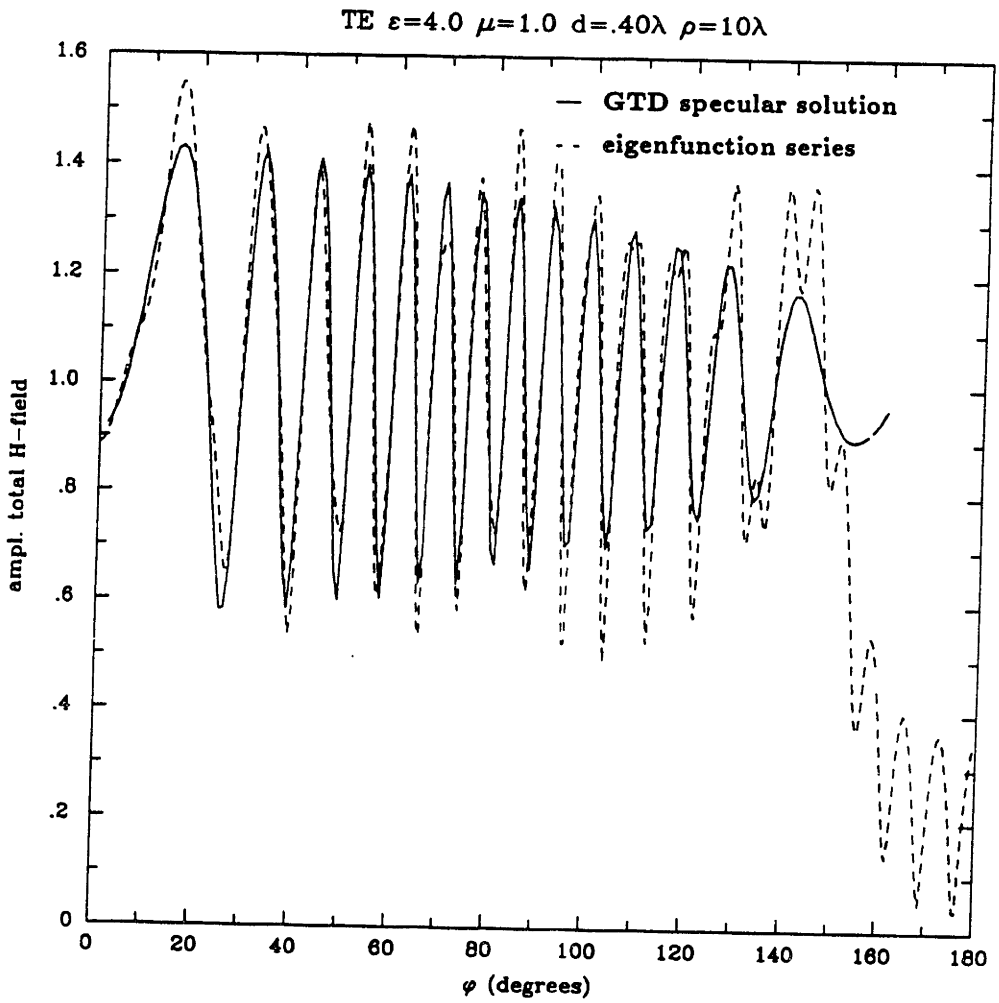

Figure 3.10 Comparison of GTD and eigenfunction solutions–TE

CHAPTER 4

CREEPING WAVE DIFFRACTION

The creeping waves in the illuminated region and the entire radiation in the shadow region involve only the diffracted field. The diffracted rays contributing to scattering are called "creeping waves" because the rays traverse about the outer perimeter of the coating as if they were "creeping." The diffracted field both in the illuminated and shadow regions are solved using the residue series solution. The residue series solution of (2.30) is an exact expression for the total scattered field in the shadow region. Because the $\cos\nu(\phi-\pi)$ term in (2.30) is convergent within the shadow region, it is not necessary to break up the field into the dominant diffraction and multiply encircling creeping wave parts. For the illuminated region, the cosine term $\cos\nu(\phi-\pi)$ in (2.30) does not converge, but the cosine term $\cos\nu\phi$ in (3.5) does. Therefore, the residues series expression for the illuminated region is similar in form to (2.30).

The equation

$$\overline{F}^{cw} = \hat{\pi}F_0 \sum_{n=1}^{\infty} \frac{N_{\nu_n}}{[\frac{\partial}{\partial\nu}D_\nu]_{\nu=\nu_n}} \frac{\cos\nu_n\phi}{\sin\nu_n\pi} e^{i\nu_n\pi/2} H_{\nu_n}^{(1)}(k_0\rho) \tag{4.1}$$

is valid for angles within the illuminated region,

$$0 \geq \phi < \phi_{sb}$$

. The numerical computation of (4.1) requires the computation of Hankel functions of complex argument and complex order. In order to eliminate the need for such

computation, an approximate form of the residue series by Habashy [11] is presented here. The modes of the diffracted field correspond to the poles in the ν-plane in the vicinity of $k_0 b$. We first make the initial assumption that $\nu \approx k_0 b$, solve for the modal equation, and then show that this assumption is self-consistent. For the case derived here, wavelength is small compared to the dimensions of the cylinder—that is, $k_0 a \gg 1$ and $k_0 b \gg 1$. The following analysis is useful for high frequency scattering.

Expressions for N_ν and D_ν

In order to find the resonant modes, we need to find the roots for modal equation. For the TM case, the modal equation is:

$$\begin{aligned} D_\nu^m =& \mu_1 k_0 H_\nu^{(1)\prime}(k_0 b)\left[H_\nu^{(1)}(k_1 b)H_\nu^{(2)}(k_1 a) - H_\nu^{(2)}(k_1 b)H_\nu^{(1)}(k_1 a)\right] \\ & -\mu_0 k_1 H_\nu^{(1)}(k_0 b)\left[H_\nu^{(1)\prime}(k_1 b)H_\nu^{(2)}(k_1 a) - H_\nu^{(2)\prime}(k_1 b)H_\nu^{(1)}(k_1 a)\right] = 0 \end{aligned} \tag{4.2}$$

Since $\nu \approx k_0 b$ and $k_0 b \gg 1$, the following approximations by Olver [24] apply to $H_\nu^{(1)}(k_0 b)$, $H_\nu^{(1)\prime}(k_0 b)$, $H_\nu^{(2)}(k_0 b)$, and $H_\nu^{(2)\prime}(k_0 b)$ when order and argument are large and almost equal:

$$H_\nu^{(1)}(\xi) \approx 2\left(\frac{2}{\xi}\right)^{1/3} e^{-i\pi/3} Ai\left\{-(\nu-\xi)\left(\frac{2}{\xi}\right)^{1/3} e^{-i\pi/3}\right\} \tag{4.3a}$$

$$H_\nu^{(1)\prime}(\xi) \approx -2\left(\frac{2}{\xi}\right)^{\frac{2}{3}} e^{i\pi/3} Ai'\left\{-(\nu-\xi)\left(\frac{2}{\xi}\right)^{1/3} e^{-i\pi/3}\right\} \tag{4.3b}$$

$$H_\nu^{(2)}(\xi) \approx -2\left(\frac{2}{\xi}\right)^{\frac{2}{3}} e^{i\pi/3} Ai\left\{-(\nu-\xi)\left(\frac{2}{\xi}\right)^{1/3} e^{i\pi/3}\right\} \tag{4.3c}$$

$$H_\nu^{(2)\prime}(\xi) \approx -2\left(\frac{2}{\xi}\right)^{\frac{2}{3}} e^{-i\pi/3} Ai'\left\{-(\nu-\xi)\left(\frac{2}{\xi}\right)^{1/3} e^{i\pi/3}\right\} \tag{4.3d}$$

The Airy function satisfies the differential equation:

$$Ai''(\xi) = \xi Ai(\xi) \tag{4.4}$$

Since $|k_1| > |k_0|$ and $b \approx R$, the following Debye approximations [6] apply to $H_\nu^{(1)}(k_1 b)$, $H_\nu^{(1)\prime}(k_1 b)$, $H_\nu^{(2)}(k_1 b)$, $H_\nu^{(2)\prime}(k_1 b)$, $H_\nu^{(1)}(k_1 a)$, and $H_\nu^{(2)}(k_1 b)$ when order and argument are large but unequal:

$$H_\nu^{(1)}(\xi) \approx \sqrt{\frac{2}{\pi z}} e^{i\psi} \tag{4.5a}$$

$$H_\nu^{(1)\prime}(\xi) \approx \sqrt{\frac{2z}{\pi \xi^2}} e^{i\psi} \tag{4.5b}$$

$$H_\nu^{(2)}(\xi) \approx \sqrt{\frac{2}{\pi z}} e^{-i\psi} \tag{4.5c}$$

$$H_\nu^{(2)\prime}(\xi) \approx -i\sqrt{\frac{2z}{\pi \xi^2}} e^{-i\psi} \tag{4.5d}$$

where

$$z = \sqrt{\xi^2 - \nu^2}$$

$$\psi = z - \nu \cos^{-1}\left(\frac{\nu}{\xi}\right) - \frac{\pi}{4}.$$

The approximations by Olver are more powerful than Debye in that the former reduces to the latter as argument and order are no longer equal. When we substitute these asymptotic approximations, we get the results:

$$D_\nu^m = -\frac{8i}{\pi b}\left(\frac{2}{k_0 b}\right)^{1/3} e^{-i\pi/3} \frac{S_0}{\sqrt{S_0 S}} \cos(\psi_0 - \psi) \cdot \left[Ai(-a) - \left(\frac{2}{k_0 b}\right)^{1/3} \frac{\mu_1 k_0 b}{\mu_0 S_0} e^{-i\pi/3} Ai'(-a) \tan(\psi_0 - \psi)\right] = 0 \tag{4.6}$$

$$N_\nu^m = -\frac{8i}{\pi b}\left(\frac{2}{k_0 b}\right)^{1/3} e^{-i\pi/3} \frac{S_0}{\sqrt{S_0 S}} \cos(\psi_0 - \psi) \cdot \left[e^{-i\pi/3} Ai(a e^{-i\pi/3}) - \left(\frac{2}{k_0 b}\right)^{1/3} \frac{\mu_1 k_0 b}{\mu_0 S_0} Ai'(a e^{-i\pi/3}) \tan(\psi_0 - \psi)\right] \tag{4.7}$$

where

$$a = (\nu - k_0 b)\left(\frac{2}{k_0 b}\right)^{1/3} e^{-i\pi/3}$$

$$S_0 = \sqrt{(k_1 b)^2 - \nu^2}$$

$$S = \sqrt{(k_1 a)^2 - \nu^2}$$

$$\psi_0 - \psi = c + \nu b$$

$$c = S_0 - S$$

$$b = \cos^{-1}\left(\frac{\nu}{k_1 R}\right) - \cos^{-1}\left(\frac{\nu}{k_1 b}\right).$$

The identical scale factors in front of both D_ν^m and N_ν^m cancel. So for convenience, D_ν^m and N_ν^m can be redefined as:

$$D_\nu^m = Ai(-a) - \left(\frac{2}{k_0 b}\right)^{1/3} \frac{\mu_1 k_0 b}{\mu_0 S_0} e^{-i\pi/3} Ai'(-a) \tan(\psi_0 - \psi) = 0 \tag{4.8}$$

and

$$N_\nu^m = -e^{-i\pi/3} Ai(ae^{-i\pi/3}) + \left(\frac{2}{k_0 b}\right)^{1/3} \frac{\mu_1 k_0 b}{\mu_0 S_0} Ai'(ae^{-i\pi/3}) \tan(\psi_0 - \psi). \tag{4.9}$$

The chain rule is used to find $\frac{\partial D_\nu^m}{\partial \nu}$.

$$\frac{\partial D_\nu^m}{\partial \nu} = \frac{\partial D_\nu^m}{\partial a} \cdot \frac{\partial a}{\partial \nu} \tag{4.10}$$

where

$$\frac{\partial a}{\partial \nu} = \left(\frac{2}{k_0 b}\right)^{1/3} e^{-i\pi/3} \tag{4.11}$$

and

$$\frac{\partial D_\nu^m}{\partial a} = -Ai'(-a)\left[1+\frac{\mu_1\nu k_0 b}{\mu_0 S_0^3}\tan(\psi_0-\psi)+\frac{\mu_1 k_0 b}{\mu_0 S_0}\sec^2(\psi_0-\psi)\right] - \left(\frac{2}{k_0 b}\right)^{1/3}\frac{\mu_1 k_0 b}{\mu_0 S_0}e^{-i\pi/3}aAi(-a)\tan(\psi_0-\psi). \tag{4.12}$$

If we retrace the preceding steps for the TE case, we get:

$$D_\nu^e = Ai'(-a)+\left(\frac{k_0 b}{2}\right)^{1/3}\frac{\epsilon_0 k_1}{\epsilon_1 k_0}\frac{S_0}{k_1 b}e^{i\pi/3}Ai(-a)\tan(\psi_0-\psi)=0 \tag{4.13}$$

$$N_\nu^e = -e^{-i\pi/3}Ai'(ae^{-i\pi/3})-\left(\frac{k_0 b}{2}\right)^{1/3}\frac{\epsilon_0 k_1}{\epsilon_1 k_0}\frac{S_0}{k_1 b}Ai(ae^{-i\pi/3})\tan(\psi_0-\psi). \tag{4.14}$$

Equations (4.13) and (4.14) can be recast into a form similar to the TM equations.

$$D_\nu^e = Ai(-a)-\left(\frac{2}{k_0 b}\right)^{1/3}\frac{\epsilon_1 k_0 b}{\epsilon_0 S_0}e^{-i\pi/3}Ai'(-a)\tan(\psi_0-\psi-\frac{\pi}{2})=0 \tag{4.15}$$

$$N_\nu^e = -e^{-i\pi/3}Ai(ae^{-i\pi/3})+\left(\frac{2}{k_0 b}\right)^{1/3}\frac{\epsilon_1 k_0 b}{\epsilon_0 S_0}Ai'(ae^{-i\pi/3})\tan(\psi_0-\psi-\frac{\pi}{2}). \tag{4.16}$$

If we define a weighting factor $w^{m,e}$, equations (4.8-9) and (4.15-16) can be more succinctly written as:

$$D_\nu^m = Ai(-a)-w^m Ai'(-a)=0 \tag{4.17}$$

$$N_\nu^m = -e^{-i\pi/3}Ai(ae^{-i\pi/3})+w^m Ai'(ae^{-i\pi/3}). \tag{4.18}$$

$$D_\nu^e = Ai(-a) - w^e Ai'(-a) = 0 \tag{4.19}$$

$$N_\nu^e = -e^{-i\pi/3} Ai(ae^{-i\pi/3}) + w^e Ai'(ae^{-i\pi/3}). \tag{4.20}$$

where

$$w^m = \left(\frac{2}{k_0 b}\right)^{1/3} \frac{\mu_1 k_0 b}{\mu_0 S_0} e^{-i\pi/3} \tan(\psi_0 - \psi) \tag{4.21}$$

and

$$w^e = \left(\frac{2}{k_0 b}\right)^{1/3} \frac{\epsilon_1 k_0 b}{\epsilon_0 S_0} e^{-i\pi/3} (-\sec(\psi_0 - \psi)) \tag{4.22}$$

Since $-\sec\theta = \tan(\theta - \pi/2)$, then the modal equations for the TM and TE case differ only with the substitution of $\frac{\mu_1}{\mu_0}$ with $\frac{\epsilon_1}{\epsilon_0}$, and $\psi - \psi_0$ with $\psi - \psi_0 - \pi/2$.

$\frac{\partial D_\nu^m}{\partial \nu}$ can be easily deduced from (4.10) using the above substitutions:

$$\frac{\partial D_\nu^m}{\partial \nu} = \frac{\partial D_\nu^m}{\partial a} \cdot \frac{\partial a}{\partial \nu} \tag{4.23}$$

where

$$\begin{aligned}\frac{\partial D_\nu^m}{\partial a} = &- Ai'(-a)\left[1 + \frac{\epsilon_1 \nu k_0 b}{\epsilon_0 S_0^3} \tan(\psi_0 - \psi - \pi/2) + \frac{\epsilon_1 k_0 b}{\epsilon_0 S_0} \sec^2(\psi_0 - \psi - \pi/2)\right] \\ &- \left(\frac{2}{k_0 b}\right)^{1/3} \frac{\epsilon_1 k_0 b}{\epsilon_0 S_0} e^{-i\pi/3} a Ai(-a) \tan(\psi_0 - \psi - \pi/2).\end{aligned} \tag{4.24}$$

where $\frac{\partial a}{\partial \nu}$ is given in equation (4.11).

Creeping Wave Modes

If a is the root for the modal equation $D_\nu = 0$, the poles ν_n are given by

$$\nu = k_0 b + a \left(\frac{k_0 b}{2}\right)^{1/3} e^{i\pi/3} \tag{4.25}$$

and ν can be broken into real and imaginary components:

$$\nu' = \Re\{\nu\} = k_0 b + \frac{1}{2}\left(\frac{k_0 b}{2}\right)^{1/3} (a' - \sqrt{3}a'') \tag{4.26}$$

$$\nu'' = \Im\{\nu\} = \frac{1}{2}\left(\frac{k_0 b}{2}\right)^{1/3} (a'' + \sqrt{3}a') \tag{4.27}$$

The real part of ν corresponds to the phase factor of the creeping wave mode while the imaginary part corresponds to the attenuation.

For the uncoated case, the modal equations take the forms:

$$D_\nu^m = Ai(-a) = 0 \quad a = 2.338,\ 4.088,\ 5.521,\ 6.787, \ldots \tag{4.28}$$

$$D_\nu^e = Ai'(-a) = 0 \quad a = 1.019,\ 3.248,\ 4.820,\ 6.163, \ldots \tag{4.29}$$

Note that the modal equation for the uncoated case becomes identical to the coated case as $w \to 0$. For the coated case, the weighting variables w^m and w^e both contain $\tan(\psi_0 - \psi)$. When expanded to the first order term for $\delta = d/R$, then

$$\psi_0 - \psi \approx k_1 d \sqrt{1 - \left(\frac{k_0 b}{k_1 a}\right)^2} \approx k_1 d \sqrt{1 - \frac{k^0}{k_1^2}} \tag{4.30}$$

Since $\psi_0 - \psi$ is a function of d, w oscillates from $-\infty$ to ∞ periodically due to the tangent term. Assuming that our coating is lossless, we can consider some simple limiting cases.

TM case

1) For values of d such that $\tan(\psi_0 - \psi) \ll (2/k_0 b)^{1/3}$, then $w^m \approx 0$. Therefore, the modal equation D_ν^m appears as the uncoated TM equation. At this range of thickness d, the creeping waves undergo the same attenuation and phase shift as if the cylinder had no coating at all.

2) For values of d such that $\psi_0 - \psi \approx (2m-1)\pi/2$ where m is any integer, $\tan(\psi_0 - \psi)$ blows up and w^m approaches infinity. In this case, the TM modal equation appears as the TE uncoated case and has the same attenuation as a TE wave on a uncoated cylinder.

TE case

1) For values of d such that $\tan(\psi_0 - \psi) \gg (2/k_0 b)^{1/3}$, then $w^e \gg 1$. The modal equation D_ν^e appears as the uncoated TM equation. Thus the coated TE wave has the same attenuation as TM waves on an uncoated cylinder.

2) For values of d such that $\psi_0 - \psi \approx m\pi$ where m is any integer, $\tan(\psi_0 - \psi) = 0$ and $w^e = 0$. In this case, the modal equation D_ν^e is the same as the uncoated TE case.

These twofold cases for each polarization imply that as a function of d, the roots of the modal equation move from the value of a in one limiting case to the other. Since the roots of the two limiting cases are the zeros of $Ai(-a)$ and $Ai'(-a)$, then we can expect the roots a to move between the zeros of $Ai(-a)$ and $Ai'(-a)$. a_n corresponds to the n^{th} mode, which oscillates between the n^{th} zeros of $Ai(-a)$ and $Ai'(-a)$. For example, a_1 would move from 2.338 to 1.019, while a_2 would go 4.088 from 3.248.

At least for the lower order modes, a is not large because the zeros of $Ai(-a)$

and $Ai'(-a)$ are not large. Since we are discussing the high frequency limit where $k_0 b \gg 1$, we can the make the approximation:

$$k_0 b \gg \frac{1}{2}\left(\frac{k_0 b}{2}\right)^{1/3}.$$

From (4.26), it is deduced that $\nu' \approx k_0 b$ and $\nu' \gg \nu''$. So for the lower order modes, where a is not too large, our assumption that $\nu \approx k_0 b$ is self-consistent.

While the limiting cases indicate that the poles move between uncoated TM and TE values, it is clear that the first limiting cases for both TM and TE cover a wide range of values of d. On the other hand, the second limiting cases cover only discrete integer multiple values. Thus, a plot of the attenuation of either TM or TE would have long plateau at the uncoated TM level, interrupted by sharp downward jumps to the uncoated TE level.

Figures 4.1 and 4.2 show plots of the attenuation coefficient of the first three modes for the TM and TE cases, respectively. The plots graph attenuation scaled by a constant as a function of coating thickness at a frequency of 100 MHz. The coating permittivity is $\epsilon_1 = 3\epsilon_0$ and the permeability of that of free space, $\mu_1 = \mu_0$. The radius of the cylinder is approximately that of the earth's: $b = 6700$ meters. For both plots, the thickness is varied from 8.0 to 10.2 meters. The coating in this case can be used to model vegetation or other ground cover on the earth.

To generate the data for these plots, the Muller root finding algorithm was used to compute the roots of equations (4.17) and (4.19). Once the roots a_n were found, ν_n'' was calculated by equation (4.38). As expected, both the TM and TE plots show long plateau periodically interrupted by sharp downward drops which signify the switching of the values.

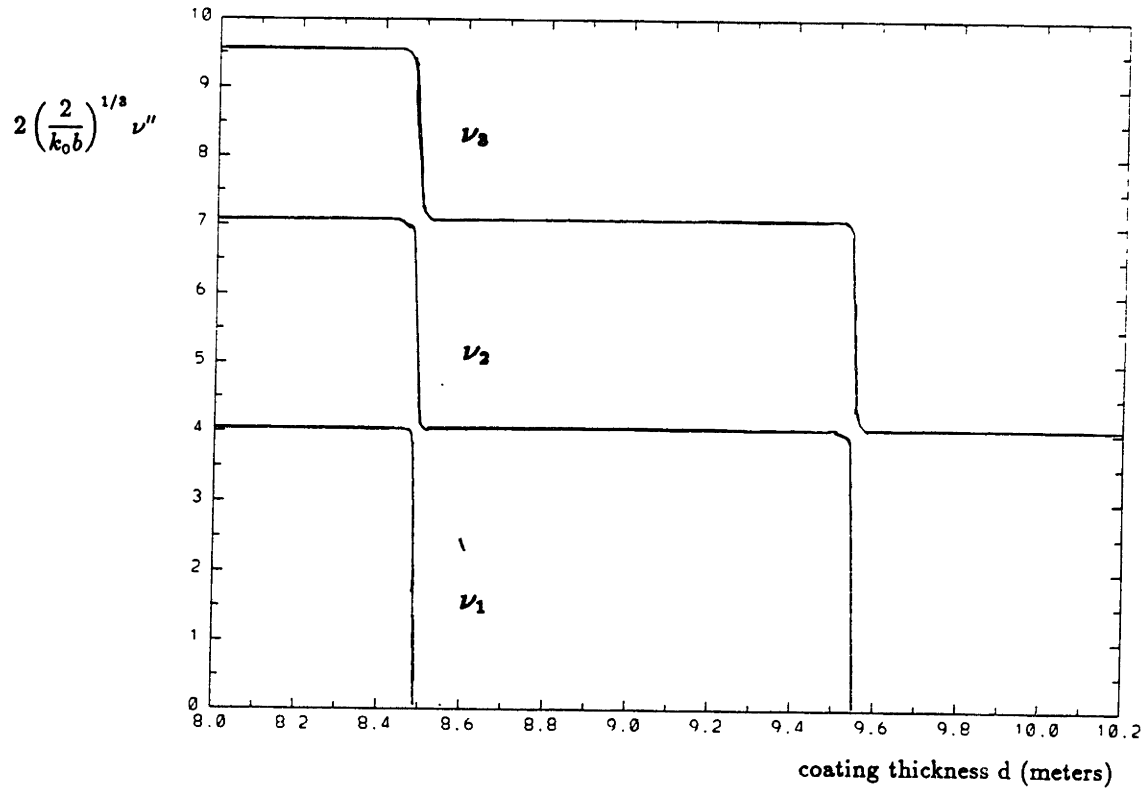

Figure 4.1 Attenuation Coefficient of TM Wave

Resonance occurs at the transition points in thickness d where $|w|$ is of order 1. At the transition points, the roots are switching from the values of the uncoated TM case and the uncoated TE case. The pass through the transition region causes the root to "drop" to a lower order level. So a root that starts at a n^{th} order mode level drops to an $n-1^{st}$ order mode. As shown in Figures 4.1 and 4.2, the roots drop to the next lower mode with each transition region from a TM plateau, to a TE descent, down to a TM plateau one order lower than originally. Thus, the root trajectories trace a downward staircase. For the zero order mode, the attenuation drops to zero, and the root "disappears." Hence, the lowest order creeping wave mode undergoes resonance.

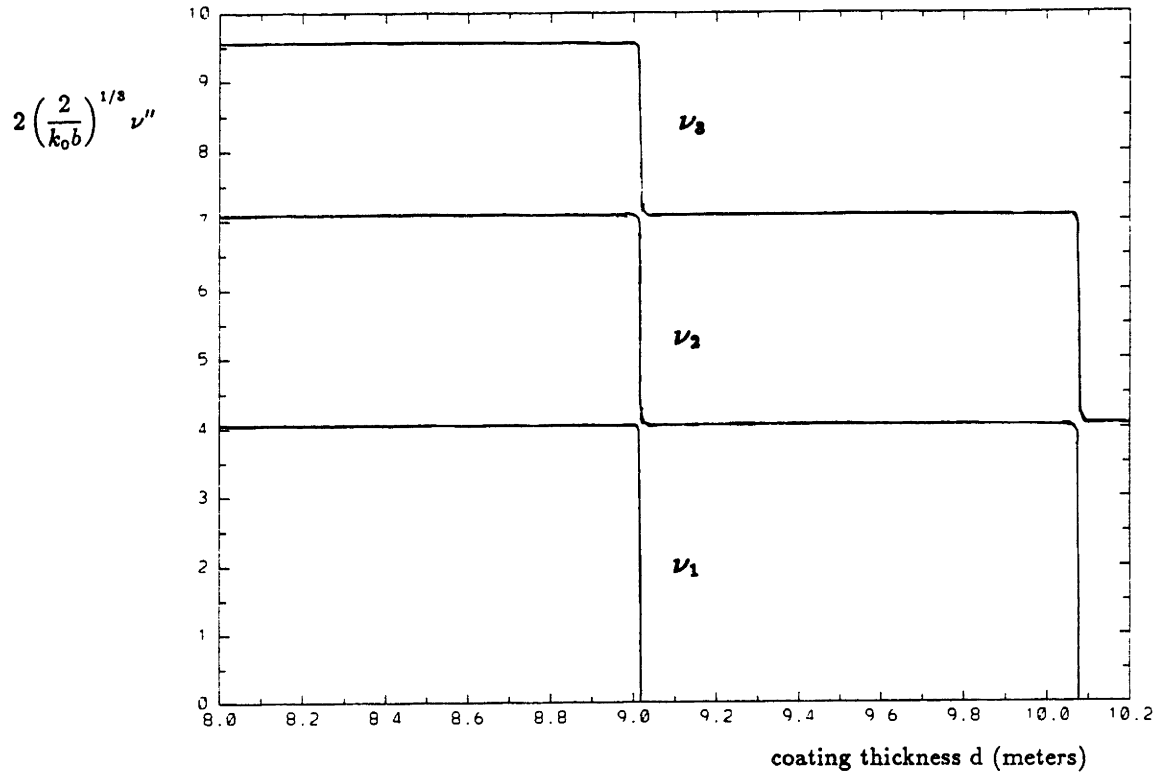

Figure 4.2 Attenuation Coefficient of TE Wave

The "staircase" plots of Figure 4.1 and 4.2 can be explained with the plot of the roots a shown in Figure 4.3. As the thickness d is varied through the resonance region, all of the roots a_n follow a curved path resembling a sine wave. When the resonance region is passed, the n^{th} order root eventually reaches the former value for the $n-1^{st}$ root. From Figure 4.3, the second order root starts at 4.1 when $d = 7.01m$ and reaches 2.34 when $d = 7.02$.

The "staircase" behavior of the roots as shown in Figures 4.1 to 4.3 are confined primarily to low loss coatings. A lossy coating will introduce a complex wavenumber k_1, which will in turn cause $\psi - \psi_0$ to become complex. Thus, the $\tan(\psi - \psi_0)$ term in

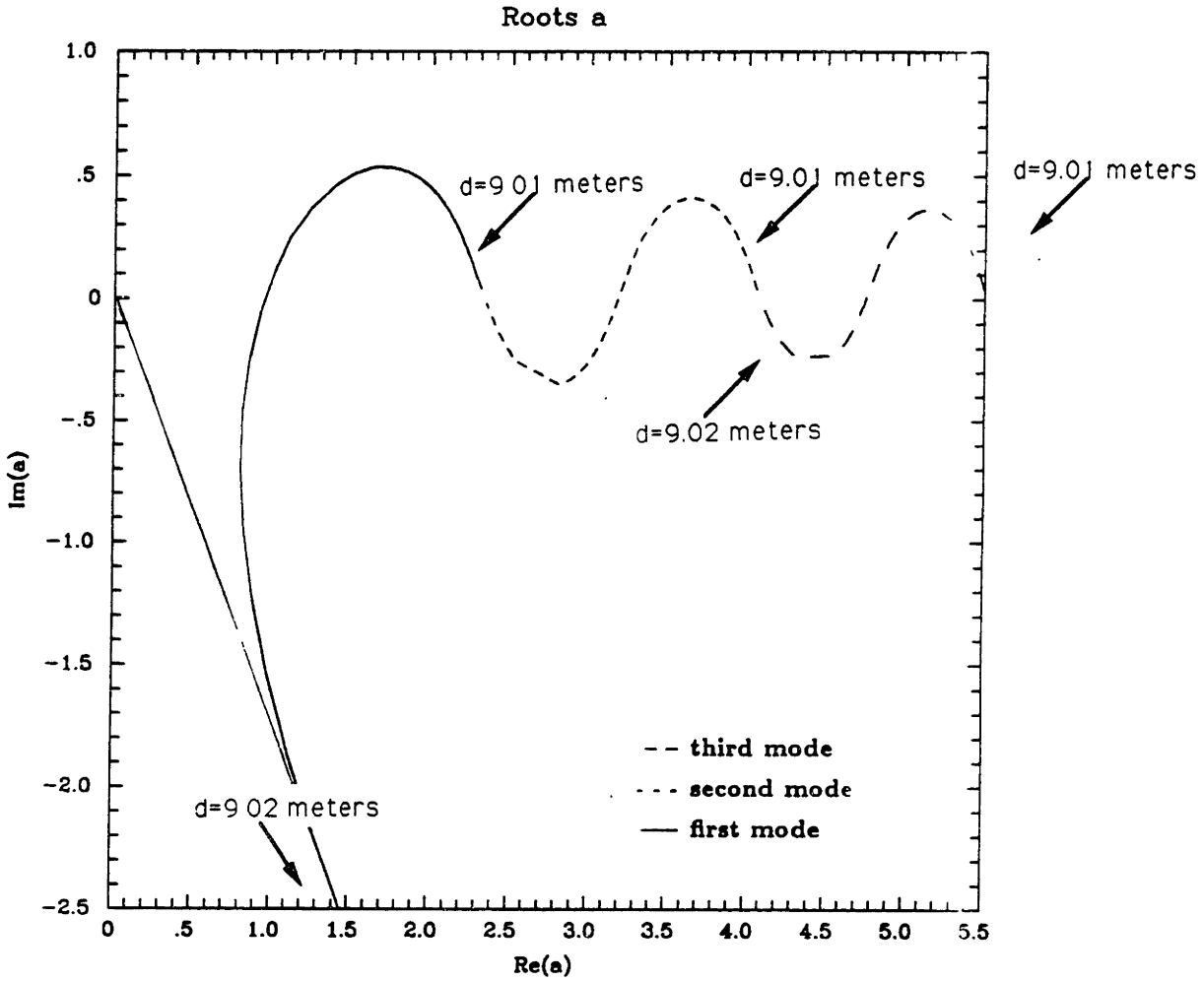

Figure 4.3 Trajectory of Root "a" with Varying Thickness

the weighting variables w will no longer exhibit an oscillatory behavior with increasing or decreasing d, and resonance will no longer occur periodically.

Furthermore, even with a lossless coating, the periodic recurrence of resonance, i.e. a sharp drop of attenuation of the lowest mode, hinges upon the fact that thickness is small compared to cylinder radius. This was assumed in the approximation made in (4.30). When the coating is comparable to cylinder radius, (4.30) no longer holds and the oscillatory behavior of w will gradually cease.

Calculation of the Creeping Wave Fields

Solving the modal equation (4.17) and (4.19) numerically yields the propagation

constants ν_n for the residue series solution (2.30). With these constants calculated, the next step is to calculate the variables N_ν and $\frac{\partial}{\partial\nu}D_\nu$. Calculation based on the exact expressions (2.14-5) and (2.23-4) requires a subroutine that computes Bessel functions with complex order and complex argument. Furthermore, the numerical derivative of D_ν must be calculated numerically. Alternatively, approximate expressions (4.10) and (4.9) can be used to calculate N_ν and $\frac{\partial}{\partial\nu}D_\nu$.

The following plots of creeping wave diffraction compare the relative accuracies of the exact and approximate expressions. This is done by plotting them with the results calculated from the eigenfunction series solutions (2.13) and (2.22), which are presumed to be the "correct" solution. Once again, the incident field is assumed to have unit amplitude, and the total field is plotted. Just as in the Chapter 3, the frequency is chosen such that $k_0 b = 20$ to ensure that both eigenfunction and residue series solution converge. The following plots will compare the creeping wave diffraction of the eigenfunction, exact residue series, and approximate residue series. The range of validity of the program CBESNY used to calculate Bessel function of complex order and complex argument limited the calculations to only the two lowest order modes. For this reason, only the first two modes of both the exact and approximate solutions for the residue series solution are used. Nevertheless, when $k_0 b = 20$, the residue series converges quite rapidly, and two modes are generally sufficient to accurately calculate the field in the deep in the shadow region.

In most of the following plots, the deep shadow region shows a good match between the eigenfunction and both residue series solutions. As expected, as observation angle ϕ approaches the shadow boundary ϕ_{sb}, the residue series no longer converges quickly. More terms become necessary, and the two terms calculated no longer supply

an accurate result. In the conditions in Figure 4.5, the cylinder is undergoing resonance, as indicated by the multiple lobes from the eigenfunction and exact residue series solutions. Unfortunately at resonance, the approximate solution tends to break down in amplitude calculation. When the attenuation coefficient of the lowest order mode drops considerably, the approximate equations for N_ν and D_ν lose their accuracy, hence the mismatch of the approximate residue solution and the eigenfunction solution. When loss is introduced in Figure 4.7, the cylinder is no longer resonant as in the lossless case of Figure 4.5. The loss tends to attenuate the wave further, and in some cases, will prevent resonance of the creeping wave. In the case of a lossy coating, the results from the exact and approximate residue series equations of Figures 4.6 and 4.7 still also give a good match with the eigenfunction solution.

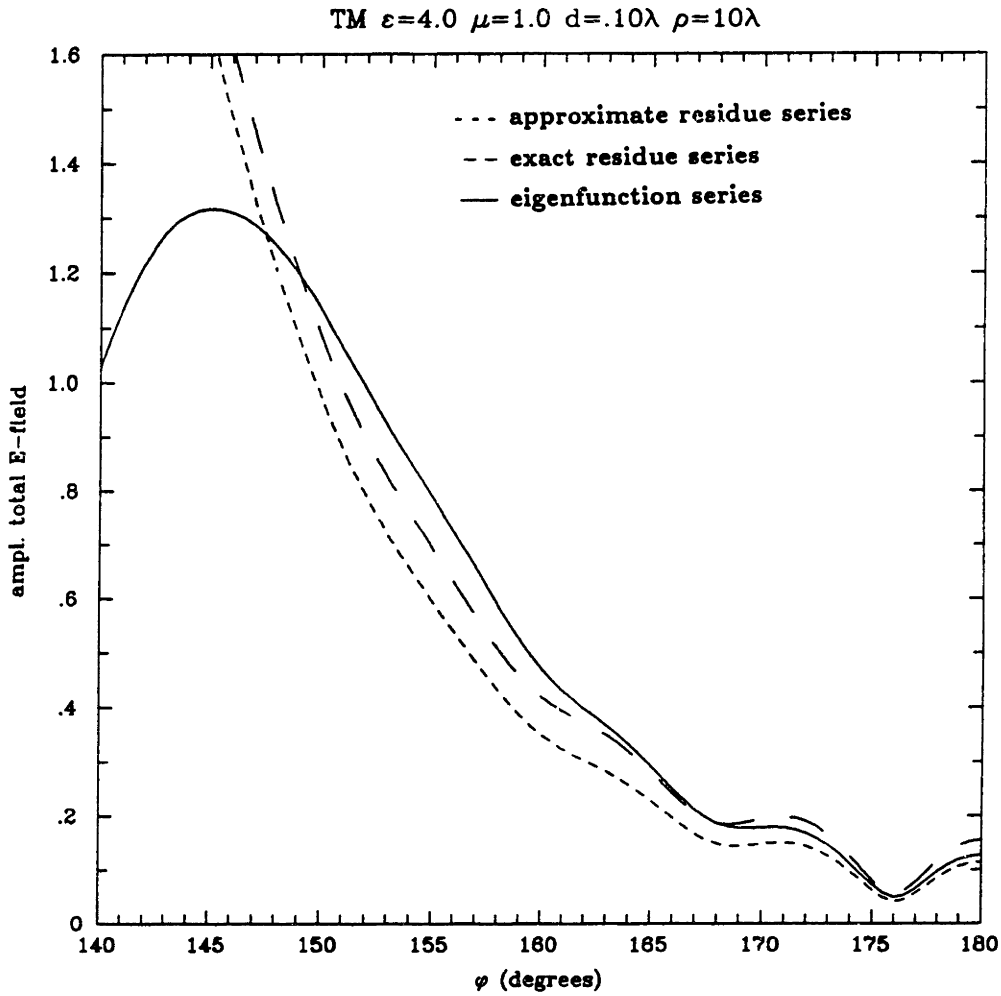

Figure 4.4 Comparison of residue series and eigenfunction solutions–TM

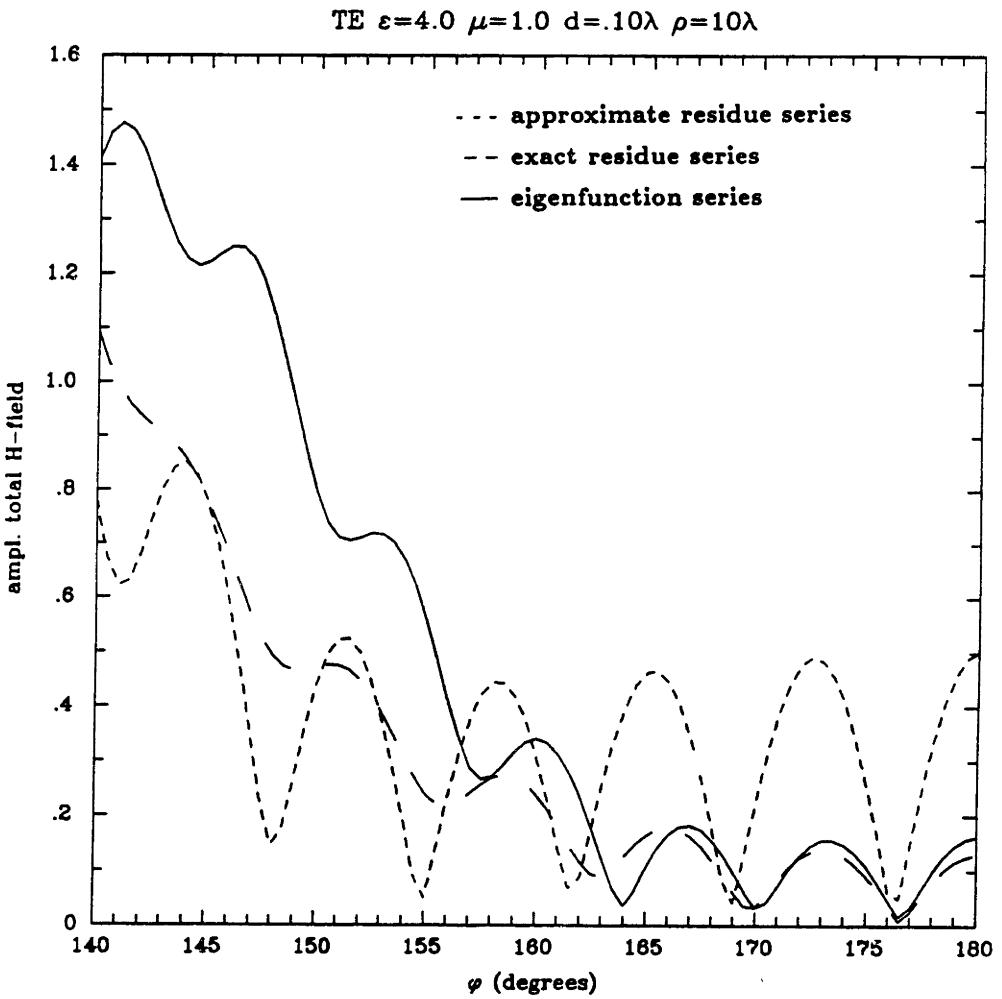

Figure 4.4 Comparison of residue series and eigenfunction solutions–TE

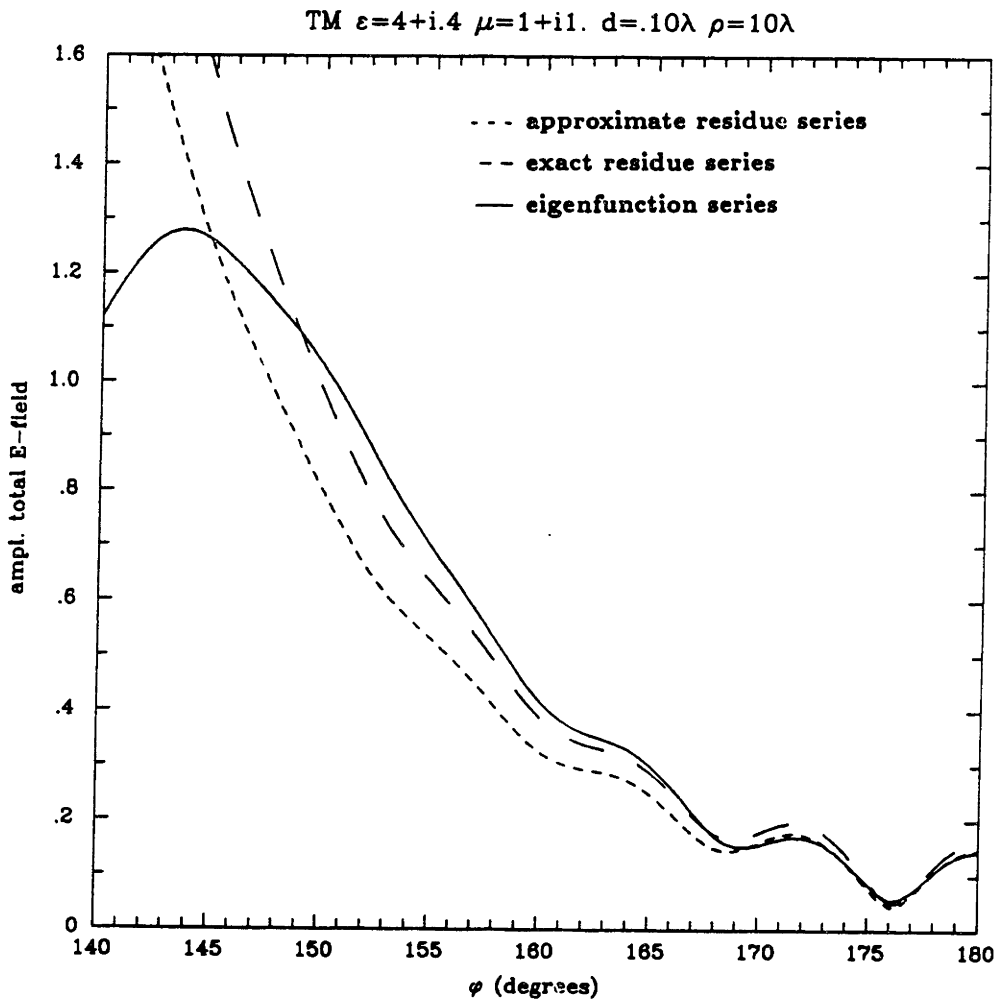

Figure 4.4 Comparison of residue series and eigenfunction solutions–TM

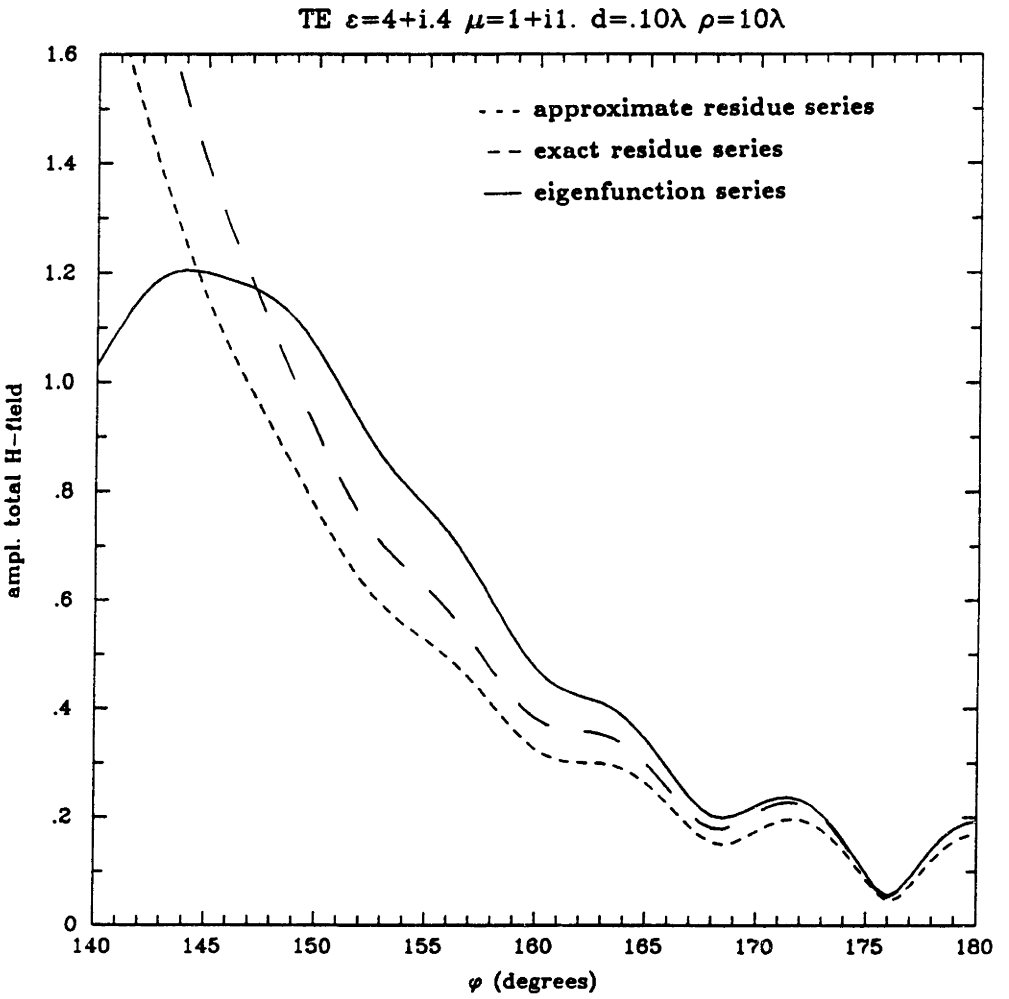

Figure 4.4 Comparison of residue series and eigenfunction solutions–TE

Ray Format for Creeping Wave

More approximations can be used to reformulate (2.30) to show the ray optics of creeping waves. For the field near the scatterer ($\rho \approx b$), we use the approximation in (4.3a) for the Hankel function in (2.30).

$$\overline{F} \approx -i\hat{z}2\pi F_0 \left(\frac{2}{k_0\rho}\right)^{1/3} e^{-i\pi/3} \sum_{n=1}^{\infty} C_{\nu_n} \left[e^{i\nu_n(\phi-\pi/2)} + e^{i\nu_n(\frac{3\pi}{2}-\phi)}\right] Ai\left\{-(\nu_n - k_0\rho)\left(\frac{2}{k_0\rho}\right)^{1/3} e^{-i\pi/3}\right\} \tag{4.31}$$

If we Taylor expand the Airy function in (4.31) around $\rho = b$ to the first order of ρ, we get the expression:

$$\overline{F} \approx -i\hat{z}2\pi F_0 \left(\frac{2}{k_0\rho}\right)^{1/3} e^{-i\pi/3} \sum_{n=1}^{\infty} C_{\nu_n} \left[e^{i\nu_n(\phi-\pi/2)} + e^{i\nu_n(\frac{3\pi}{2}-\phi)}\right] \cdot \left[Ai(-a) + k_0(\rho - b)\left(\frac{2}{k_0\rho}\right)^{1/3} e^{-i\pi/3} Ai'(-a)\right] \tag{4.32}$$

where

$$C_{\nu_n} = \frac{N_{\nu_n}}{\left[\frac{\partial D_\nu}{\partial \nu}\right]_{\nu=\nu_n}} \cdot \frac{1}{1 - e^{i\nu_n 2\pi}}$$

From the $k_0(\rho - b)$ term in (4.32), it can be concluded that the field varies linearly with ρ in the limit where $\rho \approx b$.

When $\rho > b$, the Hankel function in (2.30) can be replaced with the approximation in (4.5a):

$$\overline{F} \approx -i\hat{z}F_0 e^{-i\pi/4} \sum_{n=1}^{\infty} B_{\nu_n} \left\{ e^{i\nu_n(\phi-\pi/2)} + e^{i\nu_n(\frac{3\pi}{2}-\phi)} \right\} e^{i\gamma_{\nu_n}} \tag{4.33}$$

where

$$B_{\nu_n} = C_{\nu_n} \sqrt{\frac{2}{\pi}} (k_0^2\rho^2 - \nu_n^2)^{-\frac{1}{4}}$$

$$\gamma_{\nu_n} = \sqrt{k_0^2\rho^2 - \nu_n^2} - \nu_n \cos^{-1}\left(\frac{\nu_n}{k_0\rho}\right).$$

Expanding to the first order around $\nu = k_0 b$ gives

$$\sqrt{k_0^2\rho^2 - \nu_n^2} \approx k_0\sqrt{\rho^2 - b^2} - i\frac{\nu_n'\nu_n''}{\sqrt{k_0^2\rho^2 - \nu_n'^2}}$$

$$\nu_n \cos^{-1}\left(\frac{\nu_n}{k_0\rho}\right) \approx \nu_n' \cos^{-1}\left(\frac{b}{\rho}\right) + i\left[\nu_n'' \cos^{-1}\left(\frac{b}{\rho}\right) - \frac{\nu_n'\nu_n''}{\sqrt{k_0^2\rho^2 - \nu_n'^2}}\right]$$

Thus, the field can be simplified to:

$$\overline{F} \approx -i\hat{z}\pi F_0 e^{-i\pi/4} \sum_{n=1}^{\infty} B_{\nu_n} \left[e^{ik_0(\sqrt{\rho^2-b^2}+y_c)} e^{-\alpha_n y_c} + e^{ik_0(\sqrt{\rho^2-b^2}+y_a)} e^{-\alpha_n y_a} \right] \tag{4.35}$$

where

$$y_c = b\left[\phi - \frac{\pi}{2} - \cos^{-1}\left(\frac{b}{\rho}\right)\right]$$

$$y_a = b\left[\frac{3\pi}{2} - \phi - \cos^{-1}\left(\frac{b}{\rho}\right)\right]$$

$$\alpha_n = \frac{\nu_n''}{b}$$

Equation (4.36) gives some physical meaning into how the creeping waves propagate. As shown in Figure 4.3, y_a and y_c refer to the radial distance the waves creep on the outer interface at $\rho = b$. The phase factor in (4.35) indicates that the creeping waves propagate as if they travelled on the outer coating-air interface. The coating properties μ_1 and ϵ_1 and thickness d seem to have primary effect on the attenuation α and the amplitude B_{ν_n}. Once the rays have travelled distance y_a and y_c on the cylinder and have partially attenuated, they leave the cylinder and strike the observation point.

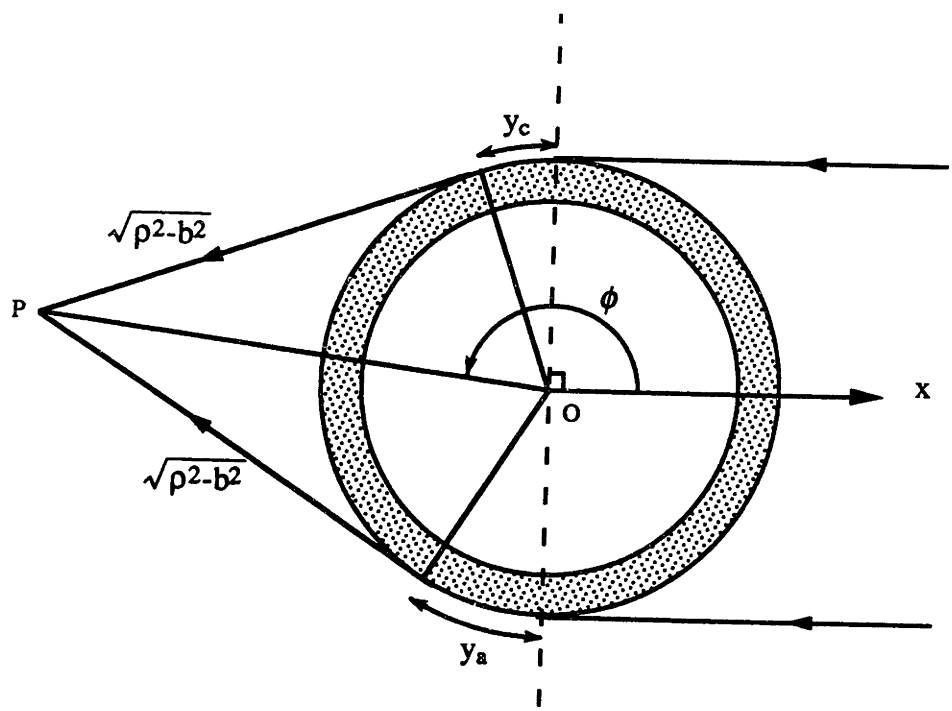

Figure 4.8 Rays of the Creeping Wave

In the region close to the cylinder ($\rho \approx b$), the field varies linearly with distance

ρ. In the far region, the phase expression for the fields indicates that the rays of the creeping waves appear to run along the outer coating perimeter without penetrating the coating. On the other hand, the field solution shows that the mode amplitudes and attenuation values are largely determined by coating properties and thickness.

CHAPTER 5

CONCLUSION

The scattering of a perfectly conducting cylinder coated with a material with permittivity ϵ and permeability μ by a plane electromagnetic wave can be solved in three forms: eigenfunction series, integral, and residue series solutions. In simplest form, the fields inside and outside the coating are expressed as sums of cylindrical harmonics. As a separable product of ρ and ϕ dependent terms, each term of the eigenfunction series is a solution to Maxwell's equation. By setting tangential $\overline{E}$ and tangential $\overline{H}$ equal at both the conducting-coating and coating-air interfaces, the weighting coefficients of each harmonic term is determined. This solution, expressed as a weighted sum of cylindrical harmonics, is called the eigenfunction series solution. Unfortunately, the eigenfunction series solution is slowly convergent for higher frequencies and is impractical for use with numerical computation. An alternate form for higher frequencies is needed.

The Watson Transformation is used to convert this slowly convergent series into a contour integral whose path of integration encircles the real axis of the ν-plane. This contour integral can be simplified into a definite integral from $-\infty$ to $+\infty$ to yield the exact integral solution. To avoid tedious numerical integration, the stationary phase approximation can be applied to yield a meaningful result. First, the integral solution can be algebraically divided into two parts. After applying stationary phase, it becomes clear that one part represents the incident field, while the other represents

the specular reflection. The specular and diffracted field can be cast into the format of Keller's Geometrical Theory of Diffraction. Two phenomena can be noted about how the coated cylinder reflects the incident rays. First, most of the specular reflection is a result of reflection from the point on the cylinder where Snell's Law is satisfied. In other words, most of the contribution to scattering occurs at the point on the cylinder surface where the angle of incident equals the angle of reflection. Second, the reflected field can be expressed as an incident field multiplied by a "spread factor." Thus, a reflection coefficient is derived. This GTD specular solution represents the dominant scattering effects in the illuminated region.

The exact integral solution can also be solved by deforming the integral path upward into a loop enclosing the upper half ν-plane. This final contour integral is solved by picking up the residues in the upper half ν-plane. The final result is called the residue series solution, which represents the scattered field as a sum of contributions of the natural modes of the structure. The residue series solution is quickly convergent because all but the first few modes have such high attenuation constants so as to render them negligible in their contribution to total scattering. Usually only a few terms are sufficient is yield an accurate result.

The residue series involves waves that propagate or "creep" around the outer perimeter of the coating. These creeping waves are analogous to the creeping waves around a perfectly conducting cylinder as investigated by Watson [33]. Similar to the Watson modes, the creeping wave modes for the coated cylinder have propagation constants lying in the vicinity of $k_0 b$. The residue series solution includes the multiply encircling creeping wave component in the illuminated region and the entire field in the shadow region. Thus, a convergent solution for high frequency scattering are obtained

via the residue series solution.

While the numerical computation of the eigenfunction and GTD specular solutions is straightforward, the computer implementation of the exact residue series solution encounters several difficulties. Before the residue series can be evaluated, the location of the poles must be calculated by solving for the roots of a transcendental equation involving the computation of cylindrical bessel functions of complex order and complex argument. Computer programs that calculate bessel functions of complex argument and complex order are rare. The only program that could be found and is used for test cases for this thesis is CBESNY by Goldstein[9]. Computation of the Regge poles are rather cumbersome in that there exists many local minima to sidetrack the root-finding procedure on the wrong path. Round-off error of the program also makes root-finding at certain coating thickness impossible. Furthermore, the range of validity of CBESNY limits root-finding to only the lowest two modes. Nevertheless, in some cases, CBESNY may provide adequate accuracy to yield some fairly good results.

The Habashy [10] method provides a good alternative to the impedance cylinder approach. With the initial assumption that the poles ν lie in the vicinity of $k_0 b$, uniform asymptotic approximations of the Hankel function are used to simplify the modal and amplitude equations in the residue series. The approximate equations involve the computation of complex Airy functions rather than Bessel functions. Thus, the transcendental equation is greatly simplified and root-finding for the Regge poles becomes considerably easier. The computation of the series coefficients also become less involved. For thin coatings, due to the behavior of the Airy functions, the Regge pole trajectories move in a periodic fashion as thickness is varied [11]. In accordance with Wang's impedance model, the movement of the Regge poles as predicted by Habashy's

formulation imply that cylinders with thin coatings may be accurately modelled as impedance cylinders. The Habashy algorithm yields fairly good results except at resonance, where some of the asymptotic approximations of the Hankel functions are no longer valid.

Upon inspection of the approximate modal equation, some limiting cases become apparent. For both the TE and TM modes, as a function of coating thickness, plateau at TE uncoated levels, interrupted by periodic sharp drops that cut through to the TM uncoated levels. The resonant creeping wave modes can be calculated by finding the roots to the modal equation numerically. The results of one such calculation are shown in plots in Figures 4.1 and 4.2. The plateau at the TE uncoated levels are confirmed by the plots, but at the transition points, the roots drop to the next lower order mode level, tracing the path of downward staircases.

Finally, expression for the fields in the shadow region is obtained. In the region close to the cylinder ($\rho \approx b$), the field varies linearly with distance ρ. In the far region, the phase expression for the fields indicates that the rays of the creeping waves appear to run along the outer coating perimeter without penetrating the coating. On the other hand, the field solution shows that the mode amplitudes and attenuation values are largely determined by coating properties and thickness.

To verify the theory, the various exact and approximate scattering solutions were implemented on computer code. Results from programs which calculate the bistatic plane wave scattering based upon the eigenfunction solution, the GTD specular reflection solution (illuminated region), and the residue series solution (shadow region) are compared. Comparison of the scattering solutions of the approximate and exact solutions indicate that in most cases the approximate solution derived herein are valid.

Only in deep resonance does the approximate residue series solution lose its accuracy. Also, test cases also show that the GTD specular and eigenfunction solutions give well matched results in the illuminated region.

Future Work

Future work can be done to find an alternate approximate solution that will yield accurate results in the deep resonance condition. More accurate asymptotic expansions for Hankel functions than those used in Chapter 4 may produce a better approximate formulation for residue series. Other relevant future work include extending the approximate solution to plane wave incident at oblique angles.

REFERENCES

[1] Abramowitz, M., Stegun, I. A. (1984), *Pocketbook of Mathematical Functions*, Verlag Harri Deutsch.

[2] Bowman J. J., Senior, T. B. A. and Uslenghi, P. L. E. (1987), *Electromagnetic and Acoustic Scattering by Simple Shapes*, Hemisphere Publishing.

[3] Coolidge, J. L.(1908), "The Continuity of the Roots of an Algebraic Equation," *Annals of Math.*, Vol. 9, pp. 116-8.

[4] Elliot, R. S. (1955), "Azimuthal Surface Waves on Circular Cylinders," *Journal of Applied Physics* , Vol. 26, pp. 368-76.

[5] Erdelyi, A. (1953), *Higher Transcendental Functions*, McGraw-Hill.

[6] Felsen, L. B., Marcuvitz, N. (1973), *Radiation and Scattering of Waves*, Prentice-Hall.

[7] Fock, V. A. (1965), *Electromagnetic Diffraction and Propagation Problems*, Pergamon Press, New York.

[8] Franz, W. (1957), *Theorie der Beugung elektromagnetischer Wellen*, Springer-Verlag, Berlin.

[9] Goldstein, M., Abramson, H., FORTRAN program CBESNY, Courant Institute of Mathematical Sciences, New York University, New York, NY 10012.

[10] Gradshteyn, I., Ryzbik, I. (1980), *Table of Integrals, Series, and Products*, Academic Press.

[11] Habashy, T. M. (1984), *Radiation and Scattering of Electromagnetic Waves in Layered Media*, M.I.T. PhD Thesis.

[12] Helstrom, C. W. (1962), "The Mathematics of Scattering from a Dielectric-Coated Cylinder", *Westinghouse Research Report* 62-106-521-R2.

[13] Helstrom, C.W. (1963), "Scattering from a Coated Cylinder with a Dielectric Material", *Electromagnetic Theory & Antennas*, E.C. Jordan.

[14] James, G. L. (1976), *Geometrical Theory of Diffraction for Electromagnetic Waves*, Peter Peregrinus Ltd.

[15] Kato, S., Wang, N., (1988), "A GTD Solution to Scattering of Plane Waves at Oblique Incidence by a Dielectric Coated Circular Cylinder," *Ohio State Electro-Science Report* No. 717374-6.

[16] Keller, J. B. (1962), "Geometrical Theory of Diffraction," *Journal of the Optics Society of America*, 52, pp. 116-30.

[17] Keller, J. B. (1956), "Diffraction by a Convex Cylinder," *IEEE Transactions on Antennas and Propagation* , AP-24, pp. 312-21.

[18] Kim, H., Wang, N., (1987) "High Frequency Analysis of EM Scattering from a Circular Conducting Cylinder with Dielectric/Ferrite Coating," *Ohio State ElectroScience Report* No. 717674-4.

[19] Knott, E. F., Shaeffer, J. F., Tuley, M. T. (1986), *Radar Cross Section: its Prediction, Measurement, and Reduction*, Artech House.

[20] Kodis, R. D. (1961), "On the Theory of Diffraction by a Composite Cylinder," *J. Res. Nat. Bur. Stan., D. Radio Prop.*, Vol. 65D, No. 1.

[21] Kong, J. A. (1986), *Electromagnetic Wave Theory*, Wiley & Sons.

[22] Lim, J. S. (1988), *Two-Dimensional Signal and Image Processing*, Prentice-Hall.

[23] Logan, N. A., and Yee, K. S.(1964), "A Simple Expression for Propagation Constants Associated with a Reactive Convex Surface," *IRE Transactions on Antennas and Propagation* , AP-12, pp. 764-6.

[24] Olver, F. W. J. (1954), "The Asymptotic Expansion of Bessel Functions of Large Order," *Phil. Trans. Roy. Soc.* 247A, No. 930, pp. 328-68.

[25] Paknys, R. J., Wang, N. (1987), "High Frequency Surface Field Excited by a Magnetic Line Source on an Impedance Cylinder," *IEEE Transactions on Antennas*

and Propagation , AP-35, pp. 293-8.

[26] Paknys, R. J., Wang, N. (1986), "Creeping Wave Propagation Constants and Modal Impedance for a Dielectric Coated Cylinder," *IEEE Transactions on Antennas and Propagation* , AP-34, No. 5., pp. 674-80.

[27] Paknys, R. J. (1985), *High Frequency Surface Fields Excited by a Line Source on a Dielectric Coated Cylinder*, Ohio State Ph.D. Thesis.

[28] Pathak, P.H. (1979), "An Asymptotic Analysis of the Scattering of Plane Waves by a Smooth Convex Cylinder," *Radio Science*, Vol. 14, No. 3. May-June, pp. 419-35.

[29] Pathak, P., Wang, N. (1981), "Ray Analysis of Mutual Coupling Between Antennas on a Convex Surface", *IEEE Transactions on Antennas and Propagation* , AP-29, No. 6. pp. 911.

[30] Press, W., Flannery, B., Teukolsky, S., Vetterling, W. (1986), *Numerical Recipes: The Art of Scientific Computing*, Cambridge University Press.

[31] Shatz, M. P. and Polychronopoulos G.H. (1988), "An Improved Spherical Earth Diffraction Algorithm for SEKE," *MIT Lincoln Lab Report* CMT-111

[32] Streifer, W. (1964), "Creeping Wave Propagation Constants for Impedance Boundary Conditions," *IEEE Transactions on Antennas and Propagation* , AP-12, pp. 764-6.

[33] Tyras, G. (1969), *Radiation and Propagation of Electromagnetic Waves*, Academic Press.

[34] Wait, J. R. (1960), "On the Excitation of Electromagnetic Surface Waves on a Curved Surface," *IRE Transactions on Antennas and Propagation* , pp. 445-8.

[35] Wait, J. R. (1959), *Electromagnetic Radiation from Cylindrical Structures*, Pergamon Press.

[36] Wang, N., (1985), *Electromagnetic Scattering from a Dielectric Coated Cylinder, IEEE Transactions on Antennas and Propagation* , AP-33, pp. 960-3

[37] Wang, N., (1982), "Regge Poles, Natural Frequencies, and Surface Wave Resonance of a Circular Cylinder with a Constant Surface Impedance," *IEEE Transactions on Antennas and Propagation* , AP-30, pp.1244-7.

[38] Wu, T. T. (1956), "High Frequency Scattering," *The Physical Review*, Vol. 104, No. 5, pp. 1201-12.

```
c This program calculates the eigenfunction solution
c    of scattering of
c    infinite cylinders.  Link with Bessel routines and COEFF,FIELD
c    Data about the cylinder
c    is inserted into the file EIGEN.DATA.   Results are written in EIGEN.OUT.

c         Main Program
          real k0,a,d,b,rho
          real phi,phi1,phi2,dphi
          complex epsr,mur,k1
          complex u,znorm,field,inc,fieldi,fieldt
          common /cyl/ znorm,k0,k1,b,a,ipol,nconv,nconv1,nconv2,inear
          complex*16 c(100)
          complex permr
          common /cyl1/ permr
          complex*16 ampl(20),nus(20)
          common /cyl3/ ampl,nus

          open(unit=1,status='old',file='eigen.data')
          open(unit=2,status='new',file='eigen.out')

          read(1,*) k0,epsr,mur,ipol
          read(1,*) b,d,rho
          read(1,*) phi1,phi2,nphi,nconv,nconv1,nconv2
          read(1,*) igtd,iinc,inear

c         open(unit=4,status='new',file='eigen2.out')

          a = b-d
          u=(.0,1.0)

          k1 = k0*sqrt(epsr*mur)
          znorm = sqrt(mur/epsr)
          if (ipol .eq. 0) then
            permr = mur
           else
            permr = epsr
           endif

c  Compute the coefficients
          if (igtd .ne. 1) call coeff(rho,c)

          dphi = (phi2-phi1)/(nphi-1)
c         if (igtd .eq. 0) write(2,*) nphi

          inc = 0
          if (igtd .eq. 0) then
             do np=1,nphi
              phi=phi1 + dphi * (np-1)
              if (iinc .ne. 0) inc = exp(-u*k0*rho*cosd(phi))
              fieldt = field(phi,c,rho)+inc
```

```
            write(2,*) phi,abs(fieldt)
c           write(4,*) phi,arg(fieldt)
           end do
         elseif (igtd .eq. 1) then
           do np=1,nphi
            phi = phi1 + dphi*(np-1)
            thi = phi
            phix = 2*thi - asind(b/rho*sind(thi))
            if (iinc .ne. 0) inc = exp(-u*k0*rho*cosd(phix))
            fieldt = fieldi(thi,c,rho)+inc
            write(2,*) phix,abs(fieldt)
c           write(4,*) phix,arg(fieldt)
           end do
         else
           do np=1,nphi
            phi = phi1 + dphi*(np-1)
            thi = phi
            phix = 2*thi - asind(b/rho*sind(thi))
            if (iinc .ne. 0) inc = exp(-u*k0*rho*cosd(phix))
            fieldt = fieldi(thi,c,rho)+field(phix,c,rho)+inc
            write(2,*) phix,abs(fieldt)
c           write(4,*) phix,arg(fieldt)
           end do

         endif
100      continue

        close(unit=1)
        close(unit=2)
        close(unit=3)
        end

        function arg(z)
        complex z

        phi = aimag(log(z))
c       arg = phi*45./atan(1d0)
        arg = phi
        return
        end
```

```
c  The following subroutines COEFF and FIELD are to be linked with the
c        main program to calculate the eigenfunction solution for a
c        coated cylinder.
c  This subroutine calculates the coefficients for the subroutine FIELD.
c  It also requires the subroutine BESSEL to supply the desired
c        values for the Bessel functions.

      subroutine coeff(rho,bc)
      real rho,phi,phir,k0
      complex znorm,k1
      common /cyl/ znorm,k0,k1,b,a,ipol,nconv,nconv1,nconv2
      complex*16 arg,jn(100),yn(100),jpn(100),ypn(100)
      complex*16 jn1(100),yn1(100),jpn1(100),ypn1(100)
      complex*16 u,d(100),c(100)
      complex*16 bc(1)
      complex*16 h1,h2,h1p,h2p
      real pio2

      open(unit=3,status='new',file='eigen1.out')

      write(6,220)
220    format(/,' Computing coated eigenfunc solution')

      u=(.0,1.0)

      arg=k1*a
      call bessel(arg,nconv,jn,yn,jpn,ypn)

      arg=k1*b
      call bessel(arg,nconv,jn1,yn1,jpn1,ypn1)

      do 100 i=1,nconv2
      if (ipol .eq. 0) then
         c(i)=-u/znorm*(jn(i)*ypn1(i)-yn(i)*jpn1(i))
     +              / (jn(i)*yn1(i)-yn(i)*jn1(i))
       else
         c(i)=-u*znorm*(jpn(i)*ypn1(i)-ypn(i)*jpn1(i))
     +          / (jpn(i)*yn1(i)-ypn(i)*jn1(i))
       end if
100    continue

      arg = k0*b
      call bessel(arg,nconv1,jn,yn,jpn,ypn)

      do 200 i=1,nconv2
      h1   = jn(i) + u*yn(i)
      h1p  = jpn(i) + u*ypn(i)
      d(i) = -(jpn(i) - u*c(i)*jn(i)) / (h1p - u*c(i)*h1)
200    continue

      arg = k0*rho
```

```
      call bessel(arg,nconv,jn,yn,jpn,ypn)

      h1 = jn(1) + u*yn(1)
      bc(1) = d(1)*h1

      i=1
      write(3,50) i,bc(1)
50    format(' c(',i2,')=',2g11.4)

      do 300 i=2,nconv2
        h1 = jn(i) + u*yn(i)
        bc(i) = 2.* d(i)*h1 *(-u)**(i-1)
        write(3,50) i,bc(i)
300   continue

      close(unit=3)
      return

      end

c  The following function calculates the fields based upon the coefficients
c     computed by the subroutines COATED1 or UNCOATED1.  The arguments are
c     the distance RHO, the angle PHI, and the coefficients C.

      complex function field(phi,c,rho)
      real phi,phir,rho,k0
      complex*16 c(1)
      complex znorm,k1,u
      common /cyl/ znorm,k0,k1,b,a,ipol,nconv,nconv1,nconv2

      u = (.0,1.0)
      phir = 3.14159265/180.*phi
      field=0
      field = c(1)
      do i=2,nconv2
      field = c(i)*cos((i-1)*phir) + field
      end do
      return
      end

      complex function fieldi(thi,c,rho)
      real thi,rho
      complex*16 c(1)
      return
      end
```

```
c This program calculates the eigenfunction solution
c    of scattering of infinite uncoated cylinders.
c    Link with Bessel routines and COEFF,FIELD
c    Data about the cylinder
c    is inserted into the file EIGEN.DATA.   Results are written in EIGEN.OUT.

c         Main Program
          real k0,a,d,b,rho
          real phi,phi1,phi2,dphi
          complex epsr,mur,k1
          complex u,znorm,field,inc,fieldi,fieldt
          common /cyl/ znorm,k0,k1,b,a,ipol,nconv,nconv1,nconv2,inear
          complex*16 c(100)
          complex permr
          common /cyl1/ permr
          complex*16 ampl(20),nus(20)
          common /cyl3/ ampl,nus

          open(unit=1,status='old',file='eigen.data')
          open(unit=2,status='new',file='eigen.out')

          read(1,*) k0,epsr,mur,ipol
          read(1,*) b,d,rho
          read(1,*) phi1,phi2,nphi,nconv,nconv1,nconv2
          read(1,*) igtd,iinc,inear

c         open(unit=4,status='new',file='eigen2.out')

          a = b-d
          u=(.0,1.0)

          k1 = k0*sqrt(epsr*mur)
          znorm = sqrt(mur/epsr)
          if (ipol .eq. 0) then
            permr = mur
           else
            permr = epsr
           endif

c  Compute the coefficients
          if (igtd .ne. 1) call coeff(rho,c)

          dphi = (phi2-phi1)/(nphi-1)
c         if (igtd .eq. 0) write(2,*) nphi

          inc = 0
          if (igtd .eq. 0) then
             do np=1,nphi
              phi=phi1 + dphi * (np-1)
              if (iinc .ne. 0) inc = exp(-u*k0*rho*cosd(phi))
              fieldt = field(phi,c,rho)+inc
```

```
            write(2,*) phi,abs(fieldt)
c           write(4,*) phi,arg(fieldt)
          end do
        elseif (igtd .eq. 1) then
          do np=1,nphi
           phi = phi1 + dphi*(np-1)
           thi = phi
           phix = 2*thi - asind(b/rho*sind(thi))
           if (iinc .ne. 0) inc = exp(-u*k0*rho*cosd(phix))
           fieldt = fieldi(thi,c,rho)+inc
           write(2,*) phix,abs(fieldt)
c          write(4,*) phix,arg(fieldt)
          end do
        else
          do np=1,nphi
           phi = phi1 + dphi*(np-1)
           thi = phi
           phix = 2*thi - asind(b/rho*sind(thi))
           if (iinc .ne. 0) inc = exp(-u*k0*rho*cosd(phix))
           fieldt = fieldi(thi,c,rho)+field(phix,c,rho)+inc
           write(2,*) phix,abs(fieldt)
c          write(4,*) phix,arg(fieldt)
          end do

        endif
100     continue

      close(unit=1)
      close(unit=2)
      close(unit=3)
      end

      function arg(z)
      complex z

      phi = aimag(log(z))
c     arg = phi*45./atan(1d0)
      arg = phi
      return
      end
```

```
      ratioy = yn(nord+1)/ynn
      ratioj = jn(1)/jn0

c If ratioj=1.0, then Jn(z) values are good.  If ratioy=1.0 Yn(z) values
c    are good.
      write(6,300) arg1,nord-1,ratioj,ratioy
300    format(' arg=',2f8.3,'  ord=',i3,/,' ratj=',2g11.4,' raty=',2g11.4)

      write(6,301) jn(1),yn(nord+1)
301    format(' jn0=',2g11.4,'  ynn=',2g11.4,/)

      return
      end
```

```
c  The following programs are linked to the main program to calculated the
c     exact eigenfunction solution for a perfectly conducting cylinder without
c     coating.

          subroutine coeff(rho,c)
          real rho,phi,phir,k0,b,a
          complex znorm,k1
          common /cyl/ znorm,k0,k1,b,a,ipol,nconv,nconv1,nconv2
          complex*16 arg,jn(100),yn(100),jpn(100),ypn(100)
          complex*16 u,d(100),c(1)
          complex*16 h1,h2,h1p,h2p
          real pio2

          u=(.0,1.0)

          arg = k0*b
          call bessel(arg,nconv1,jn,yn,jpn,ypn)

          do 200 i=1,nconv2
          if (ipol .eq. 0) then
             h1    = jn(i) + u*yn(i)
             d(i) = -jn(i)/h1
           else
             h1p = jpn(i) + u*ypn(i)
             d(i) = -jpn(i)/h1p
           endif
200       continue

          arg = k0*rho
          call bessel(arg,nconv,jn,yn,jpn,ypn)

          h1 = jn(1) + u*yn(1)
          c(1) =  d(1)*h1

          do 300 i=2,nconv2
          h1 = jn(i) + u*yn(i)
          c(i) = 2.* d(i)*h1 * (-u)**(i-1)
300       continue

          return
          end

c  The following function calculates the fields based upon the coefficients
c       computed by the subroutines COATED1 or UNCOATED1.

          complex function field(phi,c,rho)
          real phi,phir,rho,k0
          complex*16 c(1)
          complex znorm,k1,u
          common /cyl/ znorm,k0,k1,b,a,ipol,nconv,nconv1,nconv2

          u = (.0,1.0)
```

```
phir = 3.14159265/180.*phi
field=0
field = c(1)
do i=2,nconv2
field = c(i)*cos((i-1)*phir) + field
end do
return
end
```

```
c  This subroutine calculates cylindrical bessel functions Jn(z) and Yn(z)
c       and their derivatives.
c  This subroutine utilizes the bessel routines JNCOMPLEX and YNCOMPLEX
C       to calculate the bessel functions of zero and first order.
C  Recursion relations are used to calculate the higher orders and the
c       derivatives of the bessel functions.

        subroutine bessel(arg,nord,jn,yn,jpn,ypn)
        complex*16 arg,jn(1),yn(1),jpn(1),ypn(1)
        complex*16 invarg
        complex arg1,jncmplex,yncmplex
        complex jn0,ynn,ratioj,ratioy

        invarg = (1.0,.0)/arg

        arg1 = arg

c       write(6,*) 'arg= ',arg

        n = nord
        i = n+1

        jn(i) = jncmplex(arg1,n)
        jn(i+1) = jncmplex(arg1,n+1)
        jpn(i) = -jn(i+1) + n*invarg*jn(i)

        do 100 n=nord-1,0,-1
        i = n+1
        jn(i) = 2*(n+1)*invarg*jn(i+1) - jn(i+2)
        jpn(i) = -jn(i+1) + n*invarg*jn(i)
100     continue

        n = 0
        i = n+1

        yn(i) = yncmplex(arg1,n)
        yn(i+1) = yncmplex(arg1,n+1)
        ypn(i) = -yn(i+1)
        ypn(i+1) = yn(i) - invarg*yn(i+1)

        do 150 n=2,nord
        i = n+1
        yn(i) = 2*(n-1)*invarg*yn(i-1) - yn(i-2)
        ypn(i) = yn(i-1) - n*invarg*yn(i)
150     continue

c Testing for accuracy of values ...
        ynn = yncmplex(arg1,nord)
        jn0 = jncmplex(arg1,0)
```

This is a sample data file, EIGENDATA.

```
6.28319 (4.0,.0) (1.,0.) 1
3.1831 0.10 10.
0. 180. 81 2 70 30
0 1 2

k0 epsr mur ipol
b  d  rho
phi1 phi2 nphi nconv nconv1 nconv2
igtd iinc inear
(root guesses)

ipol: TM=0  TE=1
If igtd .ne. 0, then do NOT allow zero or shadow region angles to be situated
 between phi1 and phi2.

iinc: add incident field?

igtd=0:No GTD specular,  eigenfunction only OR creeping wave only
igtd=1:GTD specular only
igtd=2:GTD specular + creeping wave
```

Page 87

Page 88

```
c This program calculates the GTD specular solution of scattering of
c   infinite cylinders.  Link with COEFF for the illuminated specular
c   reflection program.
c   Data about the cylinder
c   is inserted into the file EIGENDATA.   Results are written in EIGENOUT.

c       Main Program
        real k0,a,d,b,rho
        real phi,phi1,phi2,dphi
        complex epsr,mur,k1
        complex u,znorm,field,inc,fieldi,fieldt
        common /cyl/ znorm,k0,k1,b,a,ipol,nconv,nconv1,nconv2,inear
        complex*16 c(100)
        complex permr
        common /cyl1/ permr
        complex*16 ampl(20),nus(20)
        common /cyl3/ ampl,nus

        open(unit=1,status='old',file='eigen.data')
        open(unit=2,status='new',file='eigen.out')

        read(1,*) k0,epsr,mur,ipol
        read(1,*) b,d,rho
        read(1,*) phi1,phi2,nphi,nconv,nconv1,nconv2
        read(1,*) igtd,iinc,inear

c       open(unit=4,status='new',file='eigen2.out')

        a = b-d
        u=(.0,1.0)

        k1 = k0*sqrt(epsr*mur)
        znorm = sqrt(mur/epsr)
        if (ipol .eq. 0) then
          permr = mur
         else
          permr = epsr
         endif

c  Compute the coefficients
        if (igtd .ne. 1) call coeff(rho,c)

        dphi = (phi2-phi1)/(nphi-1)
c       if (igtd .eq. 0) write(2,*) nphi

        inc = 0
        if (igtd .eq. 0) then
           do np=1,nphi
            phi=phi1 + dphi * (np-1)
            if (iinc .ne. 0) inc = exp(-u*k0*rho*cosd(phi))
            fieldt = field(phi,c,rho)+inc
```

```
            write(2,*) phi,abs(fieldt)
c           write(4,*) phi,arg(fieldt)
           end do
          elseif (igtd .eq. 1) then
           do np=1,nphi
            phi = phi1 + dphi*(np-1)
            thi = phi
            phix = 2*thi - asind(b/rho*sind(thi))
            if (iinc .ne. 0) inc = exp(-u*k0*rho*cosd(phix))
            fieldt = fieldi(thi,c,rho)+inc
            write(2,*) phix,abs(fieldt)
c           write(4,*) phix,arg(fieldt)
           end do
          else
           do np=1,nphi
            phi = phi1 + dphi*(np-1)
            thi = phi
            phix = 2*thi - asind(b/rho*sind(thi))
            if (iinc .ne. 0) inc = exp(-u*k0*rho*cosd(phix))
            fieldt = fieldi(thi,c,rho)+field(phix,c,rho)+inc
            write(2,*) phix,abs(fieldt)
c           write(4,*) phix,arg(fieldt)
           end do

         endif
100      continue

        close(unit=1)
        close(unit=2)
        close(unit=3)
        end

        function arg(z)
        complex z

        phi = aimag(log(z))
c       arg = phi*45./atan(1d0)
        arg = phi
        return
        end
```

```
c  This program calculates the specular field of a coated infinite cylinder.
c     This program is based upon equations derived by Kim & Wang using
c     stationary phase methods and GTD.  The object code is to be linked
c     with EIGENOBJ.

          complex function fieldi(thi,c,rho)
          real rho,thi,k0
          complex znorm,k1
          common /cyl/ znorm,k0,k1,b,a,ipol,nconv
          complex u,rj
          real pio2,l2,sp
          real bcosi,bsini

          u=(.0,1.0)
          bcosi = b*cosd(thi)
          bsini = b*sind(thi)

          phi = 2*thi - asind(bsini/rho)

          l2 = rho*sqrt(1. - (bsini/rho)**2) - bcosi

c         write(6,*) 'thi=',thi,' bcosi=',bcosi
          sp = sqrt(bcosi/(2*l2 + bcosi))

          call refl(rj,thi,rho)
          fieldi = exp(u*k0*(l2-bcosi))*rj*sp
          return
          end

          subroutine refl(rj,thi,rho)
          complex rj
          real thi,rho
          real k0,b,a
          complex znorm,k1,u
          common /cyl/ znorm,k0,k1,b,a,ipol,nconv
          complex cost,sinba,k1d,psi,tanpsi
          real cosi,sini

          u=(0.,1.0)
          sini = sind(thi)
          cosi = cosd(thi)
          cost = sqrt(1. - ((1.0,.0)/k1*k0*sini)**2 )

          sinba = sqrt(1. -((1.0,.0)/(k1*a)*k0*b*sini)**2 )
c         k1d = k1*(b-a)
c         psi = k1d*cost

          psi = k1*(b*cost-a*sinba)
     +          - k0*b*sini*(cost-sinba)/sqrt(1-sinba**2)

          tanpsi = sin(psi)/cos(psi)
```

```
c This program calculates the exact residue series solution of scattering of
c   infinite cylinders.  Link with Bessel routines and COEFF.
c   reflection program.
c   Data about the cylinder
c   is inserted into the file EIGEN.DATA.  Results are written in EIGEN.OUT.

c       Main Program
        real k0,a,d,b,rho
        real phi,phi1,phi2,dphi
        complex epsr,mur,k1
        complex u,znorm,field,inc,fieldi,fieldt
        common /cyl/ znorm,k0,k1,b,a,ipol,nconv,nconv1,nconv2,inear
        complex*16 c(100)
        complex permr
        common /cyl1/ permr
        complex*16 ampl(20),nus(20)
        common /cyl3/ ampl,nus

        open(unit=1,status='old',file='eigen.data')
        open(unit=2,status='new',file='eigen.out')

        read(1,*) k0,epsr,mur,ipol
        read(1,*) b,d,rho
        read(1,*) phi1,phi2,nphi,nconv,nconv1,nconv2
        read(1,*) igtd,iinc,inear

c       open(unit=4,status='new',file='eigen2.out')

        a = b-d
        u=(.0,1.0)

        k1 = k0*sqrt(epsr*mur)
        znorm = sqrt(mur/epsr)
        if (ipol .eq. 0) then
          permr = mur
         else
          permr = epsr
         endif

c  Compute the coefficients
        if (igtd .ne. 1) call coeff(rho,c)

        dphi = (phi2-phi1)/(nphi-1)
c       if (igtd .eq. 0) write(2,*) nphi

        inc = 0
        if (igtd .eq. 0) then
           do np=1,nphi
            phi=phi1 + dphi * (np-1)
            if (iinc .ne. 0) inc = exp(-u*k0*rho*cosd(phi))
            fieldt = field(phi,c,rho)+inc
```

```
            write(2,*) phi,abs(fieldt)
c           write(4,*) phi,arg(fieldt)
           end do
         elseif (igtd .eq. 1) then
           do np=1,nphi
            phi = phi1 + dphi*(np-1)
            thi = phi
            phix = 2*thi - asind(b/rho*sind(thi))
            if (iinc .ne. 0) inc = exp(-u*k0*rho*cosd(phix))
            fieldt = fieldi(thi,c,rho)+inc
            write(2,*) phix,abs(fieldt)
c           write(4,*) phix,arg(fieldt)
           end do
          else
           do np=1,nphi
            phi = phi1 + dphi*(np-1)
            thi = phi
            phix = 2*thi - asind(b/rho*sind(thi))
            if (iinc .ne. 0) inc = exp(-u*k0*rho*cosd(phix))
            fieldt = fieldi(thi,c,rho)+field(phix,c,rho)+inc
            write(2,*) phix,abs(fieldt)
c           write(4,*) phix,arg(fieldt)
           end do

         endif
100      continue

        close(unit=1)
        close(unit=2)
        close(unit=3)
        end

        function arg(z)
        complex z

        phi = aimag(log(z))
c       arg = phi*45./atan(1d0)
        arg = phi
        return
        end
```

```
c  This program calculates the creeping wave fields on a coated infinite
c       cylinder using the exact residue series solution.
c       This program is similar to those in CREEP.FOR except
c       that we use the exact equations with bessel functions instead of
c       utilizing Habashy's approximations. This is to be linked with EIGENOBJ.

      subroutine residues(roots,rho)
      complex*16 roots(1),num,den,dmodal,dmodp
      complex u,znorm,k1
      real k0,b,a
      common /cyl/ znorm,k0,k1,b,a,ipol,nconv
      complex permr,f,k1b,k1a
      real k0b,pi
      common /cyl1/ permr,f,k1b,k1a,k0b
      complex*16 ampl(20),rat,nu,nu2,dnu
      common /cyl3/ ampl
      complex arg,order,h1,bjp(100),byp(50)
      dimension bjre(100),bjim(100),yre(50),yim(50)
      complex*16 h1p0b,h10b,j1b,y1b,jp1b,yp1b,j1a,y1a,jp1a,yp1a
      complex*16 h2p0b,h20b,h1krho,sn

      u = (.0,1.0)
      pi = 4.*atan(1d0)

      do 100 i=1,nconv
        nu = roots(i)
        n = int(real(nu))
        order=nu-n+1

      arg=k0b
      call cbesny(arg,order,n,bjre,bjim,yre,yim,bjp,byp)
      h1p0b = bjp(n) + u*byp(n)
      h10b  = bjre(n)-yim(n) + u*(bjim(n)+yre(n))
      h2p0b = bjp(n) - u*byp(n)
      h20b  = bjre(n)+yim(n) + u*(bjim(n)-yre(n))

      arg=k1b
      call cbesny(arg,order,n,bjre,bjim,yre,yim,bjp,byp)
      j1b  = bjre(n) + u*bjim(n)
      y1b  =  yre(n) + u* yim(n)
      jp1b = bjp(n)
      yp1b = byp(n)

      arg = k1a
      call cbesny(arg,order,n,bjre,bjim,yre,yim,bjp,byp)
      j1a  = bjre(n) + u*bjim(n)
      y1a  =  yre(n) + u* yim(n)
      jp1a = bjp(n)
      yp1a = byp(n)

      if (ipol .eq. 0) then
```

```
        sn = (jp1b*y1a - j1a*yp1b)/(j1b*y1a - j1a*y1b)/znorm
        else
        sn = znorm*(jp1b*yp1a - jp1a*yp1b)/(j1b*yp1a - jp1a*y1b)
        end if

        den = h1p0b - sn* h10b
        num = h2p0b - sn* h20b

c        dnu = .04
        write(6,*) 'enter dnu'
        read(5,*) dnu

         nu2 = nu+dnu
         dmodp = (dmodal(nu2)-den)/dnu
         rat = num/dmodp

c       write(6,199) h1p0b,h10b,h2p0b,h20b,sn
c199     format(' h1p0b=',2g11.4,' h10b=',2g11.4,/,' h2p0b=',2g11.4,
c     +          ' h20b=',2g11.4,' sn=',2g11.4)

c       write(6,205) dmodal(nu2),den,dmodal(nu2)-den

         write(6,200) i,n,rat,num,dmodp
200      format(' mode ',i2,': n=',i3,' rat=',2g11.4,/,' nmod=',2g11.4,
     +          ' dmodp=',2g11.4)

          arg=k0*rho
          call cbesny(arg,order,n,bjre,bjim,yre,yim,bjp,byp)
          h1krho = bjre(n)-yim(n) + u*(bjim(n)+yre(n))

         ampl(i) = pi*rat/sin(nu*pi)*exp(-u*nu*pi/2.)*h1krho

100       continue
        return
        end

        complex*16 function dmodal(nu)
        complex*16 nu
        complex u,znorm,k1
        real k0,b,a
        common /cyl/ znorm,k0,k1,b,a,ipol,nconv
        complex permr,f,k1b,k1a
        real k0b
        common /cyl1/ permr,f,k1b,k1a,k0b
        dimension bjre(100),bjim(100),yre(50),yim(50)
        complex bjp(100),byp(50)
        complex arg,order
        complex*16 h1p0b,h10b,j1b,y1b,jp1b,yp1b,j1a,y1a,jp1a,yp1a
        complex*16 sn

        u=(.0,1.0)
```

```
      n = int(real(nu))-1
      order=nu-n+1

      arg=k0b
      call cbesny(arg,order,n,bjre,bjim,yre,yim,bjp,byp)
      h1p0b = bjp(n) + u*byp(n)
      h10b  = bjre(n)-yim(n) + u*(bjim(n)+yre(n))

      arg=k1b
      call cbesny(arg,order,n,bjre,bjim,yre,yim,bjp,byp)
      j1b  = bjre(n) + u*bjim(n)
      y1b  =  yre(n) + u* yim(n)
      jp1b = bjp(n)
      yp1b = byp(n)

      arg = k1a
      call cbesny(arg,order,n,bjre,bjim,yre,yim,bjp,byp)
      j1a  = bjre(n) + u*bjim(n)
      y1a  =  yre(n) + u* yim(n)
      jp1a = bjp(n)
      yp1a = byp(n)

      if (ipol .eq. 0) then
      sn = (jp1b*y1a - j1a*yp1b)/(j1b*y1a - j1a*y1b) /znorm
      else
      sn = znorm*(jp1b*yp1a - jp1a*yp1b)/(j1b*yp1a - jp1a*y1b)
      end if

      dmodal = h1p0b - sn* h10b
c     write(6,222) nu,abs(dmodal)
222    format(' nu=',2g11.4,' abs=',g10.4)

      return
      end

      subroutine coeff(rho,roots)
      real rho
      complex*16 roots(1),dmodal,dm
      dimension infer(100)
      complex u,znorm,k1
      real k0,b,a
      common /cyl/ znorm,k0,k1,b,a,ipol,nconv
      complex permr,f,k1b,k1a
      real k0b
      common /cyl1/ permr,f,k1b,k1a,k0b
      complex*16 ampl(20),nu
      common /cyl3/ ampl
      real absd
      external dmodal

      u = (.0,1.0)
```

```
      pi = 4.0*atan(1d0)

      k0b = k0*b
      k1b = k1*b
      k1a = k1*a

      epsi = .005
      nsig = 8
      kn=0
      nguess = nconv
      itmax = 150
      n = nconv


      write(6,*) 'enter guess for roots nu: '
      do i=1,n
      read(1,*) roots(i)
      write(6,105) i,roots(i)
105    format(' nu(',i2,')= ',2f8.3)
      end do

      call zanlyt(dmodal,epsi,nsig,kn,nguess,n,roots,itmax,infer,ier)

      do i=1,n
      nu = roots(i)
      dm = dmodal(nu)
      absd = abs(dm)
      write(6,100) i,nu,absd,dm
      end do
100    format(' root',i2,':  nu=',2f8.3,' abs=',g10.4,' dmod=',2g11.4)

      call residues(roots,rho)

      return
      end


      complex function field(phi,roots,rho)
      complex*16 roots(1)
      complex u,znorm,k1
      real k0,b,a
      common /cyl/ znorm,k0,k1,b,a,ipol,nconv
      complex permr,f,k1b,k1a
      real k0b
      common /cyl1/ permr,f,k1b,k1a,k0b
      complex*16 ampl(20),nu
      common /cyl3/ ampl

      u = (.0,1.0)
      pi = 4.*atan(1d0)
      phir = pi/180.* phi
```

```
      field = 0.

      do 200 i=1,nconv
c  calculating values of global variables for DMODP and NMOD subroutines
        nu = roots(i)
        field = ampl(i) * cos(nu*(phir-pi)) + field
200      continue

      return
      end

      complex function fieldi(phi,c,rho)
      complex*16 c(1)
      return
      end
```

This is a sample data file, EIGEN.DATA.

```
6.28319 (4.0,.0) (1.,0.) 1
3.1831 0.10 10.
0. 180. 81 2 70 30
1 0 2
(23,5)
(21,2)

k0 epsr mur ipol
b  d  rho
phi1 phi2 nphi nconv nconv1 nconv2
igtd iinc inear
(root guesses)

ipol: TM=0  TE=1
If igtd .ne. 0, then do NOT allow zero or shadow region angles to be situated
 between phi1 and phi2.

iinc: add incident field?

igtd=0:No GTD specular,  eigenfunction only OR creeping wave only
igtd=1:GTD specular only
igtd=2:GTD specular + creeping wave
```

```
c This program calculates the approximate residue series solution
c    of scattering of
c    infinite cylinders.  Link with Bessel routines and COEFF,FIELD, and
c    Data about the cylinder
c    is inserted into the file EIGEN.DATA.   Results are written in EIGEN.OUT.

c       Main Program
        real k0,a,d,b,rho
        real phi,phi1,phi2,dphi
        complex epsr,mur,k1
        complex u,znorm,field,inc,fieldi,fieldt
        common /cyl/ znorm,k0,k1,b,a,ipol,nconv,nconv1,nconv2,inear
        complex*16 c(100)
        complex permr
        common /cyl1/ permr
        complex*16 ampl(20),nus(20)
        common /cyl3/ ampl,nus

        open(unit=1,status='old',file='eigen.data')
        open(unit=2,status='new',file='eigen.out')

        read(1,*) k0,epsr,mur,ipol
        read(1,*) b,d,rho
        read(1,*) phi1,phi2,nphi,nconv,nconv1,nconv2
        read(1,*) igtd,iinc,inear

c       open(unit=4,status='new',file='eigen2.out')

        a = b-d
        u=(.0,1.0)

        k1 = k0*sqrt(epsr*mur)
        znorm = sqrt(mur/epsr)
        if (ipol .eq. 0) then
          permr = mur
         else
          permr = epsr
         endif

c  Compute the coefficients
        if (igtd .ne. 1) call coeff(rho,c)

        dphi = (phi2-phi1)/(nphi-1)
c       if (igtd .eq. 0) write(2,*) nphi

        inc = 0
        if (igtd .eq. 0) then
           do np=1,nphi
            phi=phi1 + dphi * (np-1)
            if (iinc .ne. 0) inc = exp(-u*k0*rho*cosd(phi))
            fieldt = field(phi,c,rho)+inc
```

```
            write(2,*) phi,abs(fieldt)
c           write(4,*) phi,arg(fieldt)
           end do
          elseif (igtd .eq. 1) then
           do np=1,nphi
            phi = phi1 + dphi*(np-1)
            thi = phi
            phix = 2*thi - asind(b/rho*sind(thi))
            if (iinc .ne. 0) inc = exp(-u*k0*rho*cosd(phix))
            fieldt = fieldi(thi,c,rho)+inc
            write(2,*) phix,abs(fieldt)
c           write(4,*) phix,arg(fieldt)
           end do
          else
           do np=1,nphi
            phi = phi1 + dphi*(np-1)
            thi = phi
            phix = 2*thi - asind(b/rho*sind(thi))
            if (iinc .ne. 0) inc = exp(-u*k0*rho*cosd(phix))
            fieldt = fieldi(thi,c,rho)+field(phix,c,rho)+inc
            write(2,*) phix,abs(fieldt)
c           write(4,*) phix,arg(fieldt)
           end do

          endif
100       continue

         close(unit=1)
         close(unit=2)
         close(unit=3)
         end

         function arg(z)
         complex z

         phi = aimag(log(z))
c        arg = phi*45./atan(1d0)
         arg = phi
         return
         end
```

```
c  This program calculates the creeping wave fields on a coated infinite
c       cylinder.  The equations were derived by Habashy and are convergent
c       for high frequencies.  This is to be linked with EIGEN.OBJ.

        subroutine residues(c,rho)
        complex*16 c(1),nmod,dmodp
        complex*16 nu,sb,sa,psi,tanpsi
        complex*16 ar,airy,airyp
        complex u,znorm,k1
        real k0,b,a
        common /cyl/ znorm,k0,k1,b,a,ipol,nconv,nconv1,nconv2,inear
        complex permr,f,k1b,k1a
        real k0b,delta,pi
        common /cyl1/ permr,f,k1b,k1a,k0b,delta
        complex*16 ampl(20),nus(20),rat,dmodal
        common /cyl3/ ampl,nus
        complex*16 eta,bb
        complex*16 z,ex
        complex arg,order,h1,bjp(100),byp(50)
        dimension bjre(100),bjim(100),yre(50),yim(50)
        real k0rho,rr

        u = (.0,1.0)
        pi = 4.*atan(1d0)

        do 100 i=1,nconv
          ar = c(i)
          nu = k0b + ar*f
          sb = sqrt(k1b**2 - nu**2)
          sa = sqrt(k1a**2 - nu**2)
          psi = delta*(sa- nu**4/sa**3/6.)
          if (ipol .ne. 0) psi = psi-2.*atan(1d0)
          tanpsi = sin(psi)/cos(psi)

          eta = nu**2/(k1a**2 - nu**2)
          bb = 1+eta-delta*(1+.5*eta*(3+.5*eta)) +delta**2*(1+.5*eta*
     +         (4*eta+eta**2))
          bb = -nu/k1a/sqrt(1+eta)*delta*bb-(1./6.)*eta**1.5*delta
          dmodp = 1+ permr*k0b*nu/sb**3*tanpsi +
     +              permr*k0b*bb/sb/cos(psi)**2
          dmodp = -airyp(-ar)*dmodp - permr*ar/f/sb*k0b*airy(-ar)*tanpsi


          ex = exp(u*pi/3.)
          z = ar/ex
          nmod =-airy(z)/ex + k0b*ex/f*permr/sb*airyp(z)*tanpsi
c         scale = -8*u/pi/b/f*sqrt(sb/sa)*cos(psi)

          write(6,422) k0b,f,permr
422     format(' k0b=',g9.2,' f=',2g9.2,' permr=',2g9.2)

          nus(i) = nu
```

```
          k0rho = k0*rho
          rat = nmod/dmodp*f

          if (inear.eq.0) then
c  Far-field solution
            ex1 = exp(u*nu*2.*pi)
            ampl(i)= exp(-u*3.*pi/4.) *sqrt(2.*pi)*rat/(1-ex1)
     +                / ((k0rho)**2-nu**2)**.25
           elseif (inear .eq. 1) then
c  Near-field solution
            ex1 = exp(u*nu*2.*pi)
            rr = (2./k0rho)**(1./3.)
            z = rr *(nu-k0rho) /exp(u*pi/3.)
            ampl(i) = -u*2.*pi*rr*exp(-u*pi/3.)*rat/(1-ex1)*airy(-z)
           elseif (inear .eq. 2) then
c  Exact solution in shadow region
            n1 = int(dreal(nu))-1
            order = nu-n1+1
            arg = k0rho
            call cbesny(arg,order,n1,bjre,bjim,yre,yim,bjp,byp)
            h1 = bjre(n1)-yim(n1) + u* (bjim(n1) + yre(n1))
            ampl(i) = pi*rat *h1 * exp(-u*nu*pi/2.) /sin(nu*pi)
           else
c  Creeping wave in illum region
            n1 = int(dreal(nu))-1
            order = nu-n1+1
            arg = k0rho
            call cbesny(arg,order,n1,bjre,bjim,yre,yim,bjp,byp)
            h1 = bjre(n1)-yim(n1) + u* (bjim(n1) + yre(n1))
            ampl(i) = 2*pi*rat *h1 * exp(u*nu*pi/2.) /sin(nu*pi)
           endif

         write(6,320) i,rat,nmod,dmodp/f
320       format(' mode',i2,': rat=',2g11.4,
     +           ' nmod=',2g11.4,' dmodp/f=',2g11.4)

100       continue

          return
          end

          complex function field(phi,c,rho)
          complex*16 c(1),airy,airyp
          complex u,znorm,k1
          real k0,b,a
          common /cyl/ znorm,k0,k1,b,a,ipol,nconv,nconv1,nconv2,inear
          complex permr,f,k1b,k1a
          real k0b,delta
          common /cyl1/ permr,f,k1b,k1a,k0b,delta
          complex*16 ampl(20),nus(20)
          common /cyl3/ ampl,nus
```

```
      complex cnu,bnu,ex1
      real phir,ray,ya,yc,alpha
      complex*16 nu,rat,h1
      complex*16 z

      u = (.0,1.0)
      pi = 4.*atan(1d0)
      phir = pi/180. * phi
      field = 0.

      do 200 i=1,nconv
c  calculating values of global variables for DMODP and NMOD subroutines
        nu = nus(i)

       if (inear .eq. 0) then
c  Far-field solution
         yc = b*(phir-pi/2.-acos(b/rho))
         ya = b*(1.5*pi-phir-acos(b/rho))
         alpha = dimag(nu)/b
         ray = sqrt(rho**2-b**2)

         field = ampl(i) * (exp(u*k0*(ray+yc)-alpha*yc) +
     +              exp(u*k0*(ray+ya) -alpha*ya)) + field

       elseif (inear .eq. 1) then
c  Near-field solution
         field = ampl(i) *(exp(u*nu*(phir-pi/2.))
     +             +exp(u*nu*(1.5*pi-phir))) + field
       elseif (inear .eq. 2) then
c  Exact solution in shadow region
         field = ampl(i) * cos(nu*(phir-pi)) + field
       else
         field = ampl(i) * cos(nu*phir) + field
       endif

200    continue

      return
      end

      subroutine coeff(rho,c)
      real rho
      complex*16 c(1)
      dimension infer(100)
      complex u,znorm,k1
      real k0,b,a
      common /cyl/ znorm,k0,k1,b,a,ipol,nconv
      complex*16 dmodal,ar
      complex permr,f,k1b,k1a
      real k0b,delta
      common /cyl1/ permr,f,k1b,k1a,k0b,delta
```

```
      complex*16 ampl(20),nus(20)
      common /cyl3/ ampl,nus
      complex nu,w
      real absd
      external dmodal
      common /weight/ w

      u = (.0,1.0)
      pi = 4.0*atan(1d0)

      k0b = k0*b
      k1b = k1*b
      k1a = k1*a

      f = (k0b/2.)**(1.0/3.0)*exp(u*pi/3.)
      delta = (b-a)/b

      epsi = .00001
      nsig = 6
      kn=0
      nguess = nconv
      itmax = 100
      n = nconv

      write(6,*)
      write(6,*) 'enter guess for roots a: '
      do i=1,n
      read(1,*) c(i)
      write(6,105) i,c(i)
105    format(' a(',i1,')=',2f11.2)
      end do

      call zanlyt(dmodal,epsi,nsig,kn,nguess,n,c,itmax,infer,ier)

      do i=1,n
      ar = c(i)
      nu = k0b + ar*f
      absd = abs(dmodal(ar))
      write(6,100) i,ar,nu,absd
      end do
100    format(' root',i2,': a= ',2f8.3,' nu=',2f9.5,' absd=',g11.4)

      call residues(c,rho)

      retur
      end

      complex*16 function dmodal(ar)
      complex*16 ar,airy,airyp
      complex u,znorm,k1
      real k0,b,a
```

```
      common /cyl/ znorm,k0,k1,b,a,ipol,nconv
      complex permr,f,k1b,k1a
      real k0b,delta
      common /cyl1/ permr,f,k1b,k1a,k0b,delta
      complex*16 nu,sa,sb,psi,tanpsi
      complex w
      common /weight/ w

      nu = k0b + ar*f
      sb = sqrt(k1b**2 - nu**2)
      sa = sqrt(k1a**2 - nu**2)
      psi = delta*(sa- nu**4/sa**3/6.)
      if (ipol .ne. 0) psi = psi-2.*atan(1d0)
      tanpsi = sin(psi)/cos(psi)

      w = -k0b*permr/f /sb * tanpsi
c     if (abs(w) .lt. 1e+8) then
        dmodal = airy(-ar) + w*airyp(-ar)
c     else
c       dmodal = airy(-ar)/w + airyp(-ar)
c     endif
      return
      end

      complex function fieldi(phi,c,rho)
      complex*16 c(1)
      return
      end
```

```
complex*16 function airy(a)
complex*16 a,f1,f2,w1,w2,f,a3,f0
complex*16 x1,x2
integer n
complex*16 m,l
complex*16 airye

if (abs(a).gt. 6) then
  airy=airye(a)
  return
  endif

x1 = .35502805389
x2 = .25881940379
a3 = a*a*a

n = 0
f1 = 1
f2 = a
f  = 1
w1 = 1
w2 = a

do while (abs(f1).gt.0.05*abs(f))
n = n+1
m = 3*n
l = m+1
f = f1
f0=f2
f1 = f1*a3/(m*(m-1))
f2 = f2*a3/(l*(l-1))

w1 = w1+f1
w2 = w2+f2

end do

airy = x1*w1 - x2*w2
return
end

complex*16 function airyp(a)
complex*16 a,f1,f2,w1,w2,f,a3,f0
complex*16 x1,x2,one
integer n
complex*16 m,l
complex*16 airyep

if (abs(a) .gt. 6) then
  airyp=airyep(a)
  return
```

```
complex*16 function airy(a)
complex*16 a,f1,f2,w1,w2,f,a3,f0
complex*16 x1,x2
integer n
complex*16 m,l

  endif

x1 = .35502805389
x2 = .25881940379
a3 = a*a*a
one = (1.0,.0)

n = 1
f1 = a*a/(2.*3.*one)
f  = f1

f2 = a3/(3.*4.*one)
f0 = f2
w1 = 3.*f1
w2 = 1 + 4.*f2

do while (abs(f1).gt.0.05*abs(f))
n = n+1
m = 3*n
l = m+1

f = f1
f0=f2

f1 = f1*a3/(m*(m-1))
f2 = f2*a3/(l*(l-1))

w1 = w1+f1*m
w2 = w2+f2*l

end do

airyp = x1*w1 - x2*w2

return
end
```

```
c  The following function calculates airy functions and derivatives for
c    large argument (|z|> 6) using asymptotic expansion.

      complex*16 function airye(a)
      complex*16 a,arg,ai1,ai2,ex
      real*8 pi,arga

      pi = 4.*atan(1.d0)

c     arga = dimag(log(a))
c     if (abs(arga/pi) .lt. .8) then
c       call airy1(a,airye)
c       return
c       endif

      arg=2.*pi*(.0,1.0)/3.
      ex = exp(arg)
      call airy1(a*ex,ai1)
      call airy1(a/ex,ai2)

      airye=-ai1*ex - ai2/ex
      return
      end

      complex*16 function airyep(a)
      complex*16 a,arg,ai1,ai2,ex
      real*8 pi,arga

      pi = 4.*atan(1.d0)

      arga = dimag(log(a))
      if (abs(arga/pi) .lt. .8) then
        call airy1p(a,airyep)
        return
        endif

      arg=2.*pi*(.0,1.0)/3.
      ex = exp(arg)
      call airy1p(a*ex,ai1)
      call airy1p(a/ex,ai2)

      airyep=-ai1/ex - ai2*ex
      return
      end

      subroutine airy1(a,ai)
      complex*16 a,ai,csi,term,sum

      csi = (2./3.)*a**1.5

      term=-(1.0,.0)/csi*15./216.
```

```
      sum = 1+term
      do 100 k=2,6
        m=6*k-1
        term= -(m-4)*(m-2)*m*term/(csi*216.*k*(2*k-1))
        sum = sum+term
100     continue

      ai= .282094791*a**(-.25)*exp(-csi)*sum

      return
      end

      subroutine airy1p(a,aip)
      complex*16 a,aip,csi,term,sum

      csi = .66666666667*a**1.5
      term=(1.0,.0)/csi*21./216.
      sum = 1+term

      do 100 k=2,6
        m=6*k+1
        term = -(m-8)*(m-4)*m*term/(csi*216.*(2*k-1)*k)
        sum = sum+term
100     continue

      aip =-.282094791*a**(.25)*exp(-csi)*sum
      return
      end

      complex*16 function airypz(a)
      complex*16 a,z,csi,term,sume,sumo
      real*8 pio4

      z = -a
      csi=.666666666667*z**1.5
      term = -(1.,.0)/csi*21./216.
      sume = 1.
      sumo = term
      k = 1

      do i=1,6
      k = k+1
      m = 6*k+1

      term = -(m-8)*(m-4)*m*term/(csi*216.*k*(2*k-1))
      sume = sume + term

      k = k+1
      m = 6*k+1
      term = (m-8)*(m-4)*m*term/(csi*216.*k*(2*k-1))
```

```
c  This subroutine calculates cylindrical bessel functions Jn(z) and Yn(z)
c        and their derivatives.
c  This subroutine utilizes the bessel routines JNCOMPLEX and YNCOMPLEX
C        to calculate the bessel functions of zero and first order.
C  Recursion relations are used to calculate the higher orders and the
c        derivatives of the bessel functions.

         subroutine bessel(arg,nord,jn,yn,jpn,ypn)
         complex*16 arg,jn(1),yn(1),jpn(1),ypn(1)
         complex*16 invarg
         complex arg1,jncmplex,yncmplex
         complex jn0,ynn,ratioj,ratioy

         invarg = (1.0,.0)/arg

         arg1 = arg

c        write(6,*) 'arg= ',arg

         n = nord
         i = n+1

         jn(i) = jncmplex(arg1,n)
         jn(i+1) = jncmplex(arg1,n+1)
         jpn(i) = -jn(i+1) + n*invarg*jn(i)

         do 100 n=nord-1,0,-1
         i = n+1
         jn(i) = 2*(n+1)*invarg*jn(i+1) - jn(i+2)
         jpn(i) = -jn(i+1) + n*invarg*jn(i)
100       continue

         n = 0
         i = n+1

         yn(i) = yncmplex(arg1,n)
         yn(i+1) = yncmplex(arg1,n+1)
         ypn(i) = -yn(i+1)
         ypn(i+1) = yn(i) - invarg*yn(i+1)

         do 150 n=2,nord
         i = n+1
         yn(i) = 2*(n-1)*invarg*yn(i-1) - yn(i-2)
         ypn(i) = yn(i-1) - n*invarg*yn(i)
150       continue

c Testing for accuracy of values ..
         ynn = yncmplex(arg1,nord)
         jn0 = jncmplex(arg1,0)
```

```
      ratioy = yn(nord+1)/ynn
      ratioj = jn(1)/jn0

c If ratioj=1.0, then Jn(z) values are good.  If ratioy=1.0 Yn(z) values
c     are good.
      write(6,300) arg1,nord-1,ratioj,ratioy
300    format(' arg=',2f8.3,'  ord=',i3,/,' ratj=',2g11.4,' raty=',2g11.4)

      write(6,301) jn(1),yn(nord+1)
301    format(' jn0=',2g11.4,'  ynn=',2g11.4,/)

      return
      end
```